Sci. J. Fac. Sci. Minufiya Univ., Vol. XIV, 2000, 179-231

Surface Delineation of Lithologies and Nomalies, Wadi Dib Area, Eastern Desert, Egypt, Using Aeroradiospectrometric Survey Data

By

Mohamed A. El-Meliegy*, Hassan M. El-Shayeb, Magdy, L. Meleik* and Ragab M. Abdel-Raheim***

*Exploration Division, Nuclear Materials Authority, P. O. Box (530) El-Maadi, Cairo, Egypt

**Geology Department, Faculty of Science, El-Minufiya University, Shebin El-Kom, Egypt

ABSTRACT

Wadi Dib area is located in the Northern part of the Eastern Desert of Egypt, between latitudes 27° 43' 30" and 27° 59' 48" N and longitudes 32° 59' 04" and 33° 29' 50" E, covering a surface area of about 1500 km^2.

The study area is mainly covered by Precambrian basement (igneous and metamorphic) rocks overlain by Phanerozoic cover sediments (Cretaceous Nubian sandstones, Tertiary sediments and Quaternary sediments). It shows a special importance as it comprises large masses of granitic rocks, which show some indication of the presence of radioactive mineralization as detected by the airborne radiospectrometric survey.

The main target of the present study is to delineate the regional geology and structure of the study area using the aeroradiospectrometric data as the main source of information. Besides, the identification of significant anomalous zones of uranium and / or thorium concentrations was carried out by searching for areas of anomalously high concentrations of uranium and / or thorium, which could be favourable sites for potential radioactive mineral deposits. This study in general revealed that :

1. *The aerospectrometric measurements recorded over the study area vary widely from 3.3 to 36.7 Ur for T. C., 0.9 to 10 ppm for eU, 3.0 to 40.3 ppm for eTh and 0.09 to 3.8 % for K. This wide variation reflects the fact that the study area is covered by rocks of various composition and is divided into four various levels of radioactivity to help differentiate the various types of rocks.*
2. *Gamma-ray spectrometric data were treated qualitatively and quantitatively by applying various techniques. Regional mapping of the different rock units of the study area has been conducted through the application of factor analysis*

technique. This technique allows the interpreter to perform a coordinate transformation of the three radioelement concentrations (eU, eTh and K), their three ratios (eU / eTh, eU / K and eTh / K) as well as the total-count (T. C.) radioactivity. It could be concluded that the first factor (F1) has an appreciable high positive loading for variables T. C., eU, eTh and K. The second factor (F2) is directly highly loaded with eU / eTh and eU/ K ratios. Meanwhile, the third factor (F3) is inversely highly loaded with eU/eTh ratio. Therefore, (F1) is called the factor of integrated radioactivity, while F2 and F3 allow the intra-rock unit differentiation. Consequently, it was possible to delineate twenty interpreted radiometric lithologic (IRL) units as a result of matching the three factor score maps with the primary geological map.

3. *The significant uraniferous anomalies were defined in three ways, the first way is done by applying the statistical treatment of the gamma-ray spectrometric data and searching for areas showing high uranium content within each rock unit. The second way is by examining the stacked profiles of eU, eU/eTh and eU/K and defining the anomalous portions. The third way is by correlating the average uranium, thorium and potassium concentrations in crustal rocks and their equivalent concentrations computed in the study area. Three mixed uranium & thorium, six uranium and five thorium anomalies were discovered over the granitic rocks, some of them are related to the surface faulting specially those having the NNW, NW, NE and ENE directions and most of the identified anomalies are confined to topographic highs.*

4. *The degree of remobilization of uranium in each rock unit is reflected from the trend variations of uranium and thorium with their ratios. This examination shows that, the high remobilization is indicated in some types of granites. This means that post-magmatic redistribution of uranium took place in this rock unit.*

5. *The application of autocovariance function technique (trend analysis) to the gamma-ray spectrometric data was carried out to define the relations between the trends of the surface structures as well as those reflecting radioelement mineralization control. From the radioactivity point of view, the Gulf of Suez-Red Sea (NW), Atalla (NNW), Trans-African (NE) and Syrian Arc (ENE) trends are the most important ones.*

INTRODUCTION

Wadi Dib area is located at the northern part of the Eastern Desert of Egypt, between latitudes 27° 43' 30" N and 27° 59' 48" N and longitudes 32° 59' 04" E and 33° 29' 50" E. It covers an area of about 1500 km^2 (Fig. 1).

This area is characterized by typically arid climate, hot during summer and cold in winter with very little or scarce rainfall and clear sky during most days of the year. Winds are occasionally strong specially during winter. Vegetation is represented by scarce desert plants, mainly around some water wells (Birs).

The study area is characterized by mild topography (Fig. 2) and is highly dissected by several longitudinal and transverse dry valleys (Wadis) mainly draining toward the Gulf of Suez. They are mostly covered with sands and gravels, while boulders and stone-blocks derived from the country rocks are accumulated at the foothills. The most famous Wadis running through Wadi (W.) Dib area are : W. Dib, W. Abu Had, W. Dara and W. El-Legayia. The majority of these Wadis are generally following the NNW, NW, NE and ENE directions. Some Wadis are controlled by faults such as W. Dib and W. Dara while few other Wadis show curvilinear shape due to physical and chemical weathering, as the case of W. Abu-Had and W. El-Legayia. The general outline of the topography of the investigated area shows that it is covered by Cretaceous and Quaternary sediments forming low hills, while the basement complex rocks form relatively high and rugged mountains. The highest and prominent peaks characterizing the study area, are those of G. (Mountain) Dara (899 m above sea level), G. Abu Shar (334 m), G. Monqul (382 m), G. El-Zeit (314 m), G. Tarbul (380 m), G. Sufr El-Dib (336 m) and G. Homrat El-Gergab (432 m).

This work deals essentially with the analysis and interpretation of the aerial gamma-ray spectrometric survey data of W. Dib area located at the Northern part of the Eastern Desert of Egypt. The study aims at the delineation of the significant radioactive zones to locate the potential radioactive targets and the elucidation of surface geological and structural setting of the area which may help in the investigation of the metallogenic provinces, if present. In order to attain this goal, the following steps were carried out in the study area.

1. Compilation of different geological and geophysical maps from various sources.
2. Qualitative and quantitative interpretation of airborne gamma-ray spectrometric survey data using various statistical methods of analysis. The interpretation serves in the field of geological mapping through the study of the relation between the airborne gamma-ray spectrometric survey data, lithology and structure.
3. Delineation of the gamma-ray spectrometric anomalies which could represent radioactive mineralized zones in the study area.
4. Integration of all the interpreted results (aeroradiospectrometry, structure and lithology), which might lead to understanding the mode of occurrence and the distribution of the radioactive minerals in the area.

The airborne geophysical survey for the study area was carried out by Aero-Service Division, Western Geophysical Company of America in 1984. It involved aeroradiospectro- metric survey over the majority of the Eastern Desert of Egypt, between the River Nile westwards and the Red Sea coast eastwards, along parallel flight lines oriented in a NE-SW direction at 1.5 km spacing, while the tie lines were flown in a NW-SE direction at 10 km intervals at a nominal flight altitude of 120 m ground clearance, using a high sensitivity 256-channel airborne gamma-ray spectrometer. The obtained airborne gamma-ray spectrometric data were reduced, compiled and finally presented in the form of contoured map (Fig. 4) at a scale of 1: 50,000 (Aero-Service, 1984).

GEOLOGICAL OUTLINES

I. LITHOLOGICAL SETTING

The succession of the different rock units is related to the Precambrian basement rocks and Tertiary sediments as well as Cretaceous Nubian Sandstones. Quaternary sediments are represented by gravels and sands, fill the Wadis and depressions. Topographically, the studied area is formed of high hills and rugged mountainsespecially the areas covered with basement rocks. The different rock units exposed in W. Dib area are chronologically grouped into the following sequence (Fig. 3), according to the classifications of El-Gaby et al. (1988 and 1990).

1. PRECAMBRIAN BASEMENT ROCKS

A. Arc Association

i. Metasediments : These rocks form together with metavolcanics the oldest rock units in the study area which are characterized by forming low country and strong dissection into low pointed hills.

ii. Metavolcanics : These rocks are generally found as flows, sills and thick sheet-like bodies normally interbedded with the First Basement (Geosynclinal) Sediments (El-Shazly, 1977). They are massive, compact and fine-grained rocks, porphyritic, non-porphyritic, sheared and schistose varieties are common near the contact with Metasediments. They include basic and intermediate varieties (meta-dolerites, meta-basalts, meta-andesites and meta-porphyrites). The second one includes acidic varieties including rhyolites, yellow tuff stones and pyroclastics. The metavolcanics in Esh El-Mallaha Range are represented by meta-dolerites forming small hills and invaded by pink granites with sharp intrusive contacts (Dardir, 1997).

iii. Diorite-Epidiorite Rocks : This complex contains rafts of metasediments and occasionally form dyke-like bodies as well as minor intrusive masses cutting the metasediments. Their contacts with both the metasediments and the granitic rocks are Irregular and not sharp. These rocks, sometimes, enclose xenoliths of intermediate-basic volcanic rocks (Francis, 1972).

iv. Older Granitoids (Grey Granites) : They include the assemblage of felsic plutonic rocks of essentially intermediate composition previously referred to as grey granites. These rocks are of grey colour, medium to coarse grained, easily weathered, usually form low lying countries and are characterized by the development of exfoliation structures. In Esh El-Mallaha Range, their composition ranges from adamellites to quartz diorites (Francis, 1972). El-Kholy (1995) reported that the older granitoids (quartz-diorites) are of two types ; the first is equigranular composed of plagioclase and hornblende, while the second is porphyritic with large phenocrysts of plagioclase embedded in coarse ground mass.

B. Intracratonic Rock Association

i. Dokhan Volcanics : These Volcanics are mainly present as rhyolite and rhyodacite with subordinate andesitic flows. Hassan and Hashad (1990) distinguished seven rock types :andesite, quartz andesite, imperial porphyry, dacite, rhyodacite, quartz trachyte and pyroclastics. The first three rock types are predominant. In Esh El-Mallaha area, Dokhan Volcanics are widely distributed. The most abundant are the pyroclastics of acid and intermediate composition (Francis, 1972). They vary in colour from black to grey and various shades of purple.

ii. Hammamat Group : The Hammamat Sediments comprise a thick succession of clastic sediments that represent the youngest unit in the layered sequences of the basement. Hassan and Hashad (1990) reported that these sediments represent the latest stage of sedimentation in the Precambrian of Egypt. The succession of the Hammamat sediments consists of a bedded series of conglomerates, greywackes and siltstones with interbedded acid volcanic rocks, tuffs and tuffaceous sediments specially near the base (Francis, 1972).

iii. Younger Granitoids : The majority of these intrusions tend either to be rounded or elongated parallel to the general direction of the Red Sea and possess relatively sharp contacts with the surrounding rocks (Francis, 1972). The younger granitic rocks outcropping in the study area are situated at Gabal Dara, Gabal Monqul, Gabal Abu-Shar, Gabal El-Zeit, North Gabal Tarbul and Gabal Homrat El-Gergab.

iv. Post-Granite Dykes : These dykes tend to be more concentrated in areas covered by older and younger granites or around such areas. They vary greatly in thickness from few cm up to more than 10 m. They are generally

rectilinear and have parallel walls. They are either vertical or steeply inclined and include (El-Gaby, 1988 and 1990) :

a- Acidic Dykes : These dykes form the oldest group of post-granite dykes. They include micro-granites, micro-granodiorites, aplites, felsites, granoporphyrites, quartz-porphyrites and dacites. They are usually of light yellow, pink and greyish colours.

b- Intermediate Dykes: These dykes together with the acidic ones are the most abundant in the area and include andesites and microdiorites. These varieties are dark coloured, varying from green to black.

c- Basic Dykes : These dykes are the least common ones in the present area, which are represented by dolerites and basalts. They are dark grey to black in colour.

2. CRETACEOUS AND TERTIARY SEDIMENTS

All the Precambrian basement rocks are overlain unconformably by Cretaceous Nubian Sandstones and Tertiary Sediments. These sediments include (El-Gaby, 1988 and 1990) :

A. Cretaceous Sediments : These sediments were subdivided into three formations, starting with the youngest :

i. Duwi Formation : It includes phosphates alternating with black shale, marl and oyster limestone.

ii. Taref Formation : It comprises fluviatile and locally aeolian sandstone, fine to medium grained with interbedded channel and soil sediments.

iii. Nubian Sandstones : They cover a large surface area in the northern part of the study area and occur at the western side of Esh El-Mallaha Range forming a belt separated from the basement rocks by a NW-trending fault.

B. Tertiary Sediments : These sediments cover a large surface area and were subdivided on the map of Conoco Coral (1988) into the following formations beginning with the youngest :

i. Shagra Formation : It includes mainly sandstones.

ii. Um-Gheig Formation : It comprises crystalline carbonate, algal, locally reefal, limestones.

iii. Um Mahara Formation : It contains reefal and algal carbonate rock with bioclastics.

iv. Thebes Formation : It comprises thinly-bedded outer-shelf chalk and chalky limestone rich in chert bands and concretions.

v. Tarawan Formation : It includes white neritic chalk and chalky limestone, containing beds of marls.

vi. Dakhla Formation : It comprises dark-grey shallow marine marl and shale with limestone intercalations.

3. QUATERNARY SEDIMENTS

Detritus, sands, gravels, pebbles, cobbles and rare boulders are distributed all over the study area and constitute the surficial cover in the main Wadis, tributaries and depressions. They are generally formed by the weathering products of the various types of rocks represented in the area.

II. STRUCTURAL SETTING

The tectonic pattern of the basement rocks of the study area is the result of combined effect of successive earth movements and is essentially polycyclic that took place since the Precambrian time, which produced various structural elements as :

A. Transverse Faults : They trend in ENE to NE direction, normal to the Red Sea general axis. They are displaced horizontally by the second group of relatively younger faults. Their major faults are those which traverse the area south of G. Monqul, G. Dara and along W. Dib.

B. Longitudinal Faults : They include all faults having NNW to NW trends. The major faults of this group are those which bound the uplifted blocks of Zeit Range, Esh El-Mallaha Range and the Red Sea hills from the east. They are step faults with their down-throws toward the north-east. Tertiary marine sediments are preserved on the down-thrown sides of these faults.

III. MINERALIZATIONS

The study area seems to be poor in its mineral resources. There are some occurrences of mineral deposits, which can be considered of economic value, such as :

A. Copper : It is found at the mouth area of W. Dara (Francis, 1972).

B. Amethyst : It is found at G. Homrat El-Gergab.

C. Gold Vein Deposits : They are found near the summit of G. Dara, W. Dib, G. Monqul and W. Abu-Had.

D. **Molybdenum** : A complex of gold-copper-molybdenum ore occurrences are encountered at one of the branches of W. Dib, G. Monqul and W. Dara (Riad et al., 1978).

E. **Marble:** True marble, metamorphosed calcareous rock occurs at W. Dib and G. El-Rukham.

METHODS AND TECHNIQUES OF INTERPRETATION

The aeroradiospectrometric techniques assist considerably in the search for uranium ores and, therefore, are of great importance to geological mapping in general and mineral exploration in particular. They can provide a means of subdividing acid igneous rocks and the sediments derived from them.

The aeroradiospectrometric data recorded at the survey altitude comes mainly from the upper few centimetres of the different rock exposures. This radioactivity is attributed to the presence of natural radioelements (U, Th and K^{40}) in varying amounts. Since different rock types give different radioactivity values, accordingly the radiospectrometric method can be used as a helpful tool for surface geological mapping. The crystalline basement rocks in the Eastern Desert of Egypt are well exposed on the surface without soil or vegetation cover. This represents one of the best conditions favourable for the application of aeroradiospectrometric method, where the screening effect of the radiation field is negligible. Consequently, the airborne radiospectrometry provides very dependable information for mineral prospection.

According to Aero-Service,1984, the difference in absolute concentrations of the three naturally-occurring radioelements as measured in a survey, whether between the different geologic units or over the same geologic unit, can be highly variable and dependent on a number of factors including the amount of outcrop, topography, ground moisture, distribution of atmospheric radon and its daughter products, horizontal and vertical distance between an exposure and a flight line and others. Significant individual uranium, thorium or potassium anomalies are dependent upon the preferential accumu-lation of these individual radioelements. Hence, the inspection of the individual K, U or Th profile traces (profiles) or contour maps may, thus lead to the interpretation of false anomalies where preferential accumulation has not occurred. The ratios of the observed radioelement concentrations are much less affected by the before-mentioned factors and as such, are better indicators of preferential accumulation. Accordingly, inspection of ratios greatly aids in uranium and/or thorium anomaly identification.

I. FACTOR ANALYSIS

Factor analysis is a multivariate statistical technique whereby the number of variables is reduced to the minimum number of independent variables which will

adequately describe the data. In many cases of geologic interest, the various measurements are not independent variables and consequently they exhibit varying degrees of correlation. This technique offers a means to reduce the complexity of a given problem by removing redundant information (Moustafa et al., 1990).

The factor analysis technique allows the geologists and geophysicists to perform a coordinate transformation from the four count rates [Potassium (K, %), equivalent Uranium (eU, ppm), equivalent Thorium (eTh, ppm) and Total Count, (T. C., Ur)] and the three ratios (eU / eTh, eU / K and eTh / K) to a system to three independent coordinates. These three coordinates are constrained to reproduce the total variance of the original data and the data can be separated into groups using the criterion that similar data points have similar coordinates. The distribution of the separated groups can be mapped for comparison with other information such as the mapped geology. This map represents a synthesis of all the radiospectrometric data. Factor analysis computation involves the following major steps :

1. Correlation Matrix

The factor analysis proper typically begins with a matrix of correlation coefficient between data variables that are being studied. This correlation matrix indicates to what extent these variables are related to each other, or overlap in what they measure.

2. Factor Extraction

Factor extraction is the second step in factor analysis which determines how many factor constructs are needed to account for the pattern of values found in correlation matrix. This process involves a numerical procedure that uses the coefficients in the R matrix to procedure factor loadings. For most factor extraction methods, these factor loadings may be thought of as correlation between the variables and the factor. Same variable might have a substantial negative loading on the factor, indicating that it is negatively correlated with the factor construct. After the first factor is extracted, its effect is removed from the correlation matrix R to produce "residual" correlations. Then, a second factor is extracted from the first factor residual correlations. If substantial values remain in the second residual correlations, a third factor must be extracted and so on, until the residuals become too small to continue.

3. Factor Rotation

The so-called rotational process in factor analysis involves finding a factor matrix into another form, that will represent an optimum set of constructs for scientific purposes. Since what is optimum for one investigator may be optimum for another, this particular phase of the factor analytic process provides a fertile

source of differences among investigators is the way they view the data. The "rotation" of the factor matrix into another form that is mathematically equivalent to the original unrotated matrix using varimax method. These factors will all be well differentiated from other. Since each is represented by a different set of variables and could be identified and described on the basic of the variables that are related to them.

II. IDENTIFICATION AND OUTLINING THE URANIFEROUS PROVINCES

There are several different ways to identify and outline potential uraniferous provinces (Saunders and Potts, 1976) :

1. By examining the average uranium values for each of the various geologic units and comparing them with the crustal average values for each rock type involved to find uranium enriched units.
2. By examining the profiles for regions of high eU, eU/ eTh and eU/K values indicating uranium enrichment over the other natural radioelements.
3. By searching the uranium anomaly maps for groups of statistically high points (computed for each individual geologic formation). The significance of each anomaly was judged for the deviations of the values within the anomaly from the mean eU/ eTh and eU/K values for each of the geologic map units involved. The deviations were expressed in units equal to the standard deviation of the appropriate data set.

The locations of those deviated from the mean for eU and eTh are represented on a point (local) anomaly map using different symbols. The absence of these symbols on a local anomaly map could be attributed to the fact that the mapped gamma-ray limit was within one standard deviation of the mean and / or those certain areas of poor counting statistics. Statistically, high uranium data points should be evaluated together with the corresponding (eU / eTh) and (eU / K) date points, geology and topography of the regions to select the most significant anomalies for further investigation.

According to Saunders and Potts (1976) the problems which can be encountered in interpretation of the airborne gamma-ray spectrometric data are generally in the form of false or misleading anomalies due to the following effects :

1. Statistical problems : These problems mean low counting rates which lead to poor statistical definitions of formations and anomalies. They can

be caused by high altitudes, low radioactive element content of surface materials, or by surface water or vegetative shielding.

2. Meteorological or erosional effects : Apparent high eU, eU / eTh and eU / K values which are confined to topographic lows can be caused by trapping of radon below an atmospheric inversion layer or possibly by radon transported down valleys by night time down slope drainage of the colder night air, or by erosional transport of natural radioactive materials from mines or outcrops. Consequently, meteorological effects have a great effect in shielding and on the distribution of radon gas or its gamma-emitting daughter products which are used to measure the amount of uranium present.

3. Errors in geologic mapping : False anomalies can be caused by map unit boundary errors or by unmapped geochemical facies changes within a given formation. Geological misclassification of data points can usually be easily identified by reference to the geologic map (the anomaly will be on or very near a map unit boundary) and the statistical parameters of the units involved. The statistically high data points will have been classified as a map unit of less mean radioactivity than that of a neighbor unit, in which the data points should have been located. Such suspected anomalies are usually small in magnitude and consist of only few points.

III. REMOBILIZATION OF URANIUM

Thorium-bearing uranium minerals resist weathering and could be transported in or out of water-saturated environments. Therefore, an oxygen-bearing atmosphere is an important factor for uranium ore formation as well as for fundamental and local uranium source formation. Oxygen-bearing ground waters are effective uranium-mobilizing agents which can leach uranium dispersed in the rocks and uranium can later be concentrated within sediments. The second stage of uranium mobilization could take place during the metamorphism of these sediments and later on through magma generation from the metamorphosed sediments. These geological processes assist the multifold mobilization of uranium, formation of its fundamental and local sources and the first economic concentration of uranium (Simov, 1988).

There is evidence that uranium is one of the first elements to become remobilized during metamorphism (Heier, 1965). That is due to the fact that uranium can easily form the soluble uranyl ion ($U02^{++}$), particularly in hexavalent state and consequently it becomes very mobile. Uranium may be transported under late-stage hydrothermal conditions and be precipitated away from thorium and potassium. The trends defined in the variations of uranium and thorium with their

ratios reflect the amount of remobilization of uranium that has occurred within the plutons.

According to Charbonneau (1982), in each rock unit, the variations of uranium and thorium with their ratios can be interpreted as :

1. If the uranium/thorium ratio increase strongly with uranium but not with thorium, post magmatic redistribution of uranium is suggested and this could be a favourable economic criterion, because uranium may have concentrated into deposits within or near the granite.
2. If the uranium / thorium ratio tends to increase some what with uranium concentration and is in dependent of thorium, it indicates that uranium has not been redistributed after intrusive event either because there was no percolation of fluids to mobilize the uranium or because the bulk of the uranium is located within stable accessory minerals.
3. I If the uranium/thorium ratio is inversely correlated with thorium and varies directly with uranium the radioelement distribution is at least in part governed by magmatic processes and the thorium was fixed in the early stages of magmatic evaluation.

QUALITATIVE INTERPRETATION OF AERORADIO-SPECTROMETRIC DATA

The qualitative interpretation of aeroradiospectrometric survey data depends mainly upon the excellent correlation, achieved previously in neighboring areas, between the general pattern of the recorded aeroradioactivity measurements and the surface distribution of the various types of rock units. The radioactivity level varies widely from one type of rock to the other and to some extent between the units of the same rock type. In some cases, the gradients are high steep and sharp enough to help delineate the lithologic boundaries. Sometimes, the radioactivity levels of these rock exposures merge into one another to various degrees without distinct separations between the different rock types and, therefore, the agreement between the lithologic and radiometric contacts is weak. In spite of these difficulties, the experience in qualitative interpretation eventually can aid to yield reliable boundaries and / or structures between the various rock types.

The relation between aerial radioactivity and geology has been interpreted according to the radiosoectrometric units inferred from the various radiospectrometric levels. This has been achieved from the experience gained in neighboring areas in the Eastern Desert of Egypt.

Surface Delineation of Lithologies and Nomalies.....

The texture of radiospectrometric contours and their radiospectrometric signatures could be an aid in the course of interpretation of the surface geology (lithology and structure) ; for example :

1. Faults, shears and certain lithological contacts may be manifested by disruption of the contours of the radiospectrometric maps. Furthermore, faults sometimes exhibit radioactive highs due to increased permeability allowing access of the migrating radon. Other faults exhibit a radioactive low because of increased leaching of radioactive minerals along fault zones.
2. Major folds can be observed by the disruption of the linear radiometric features that originate from a particular geological horizon.
3. Circular features are most commonly caused by ring complexes and intrusive rocks; where, some intrusive rocks have high radioactivity zones near the margins of the body.
4. Linear trends may indicate the strike of sedimentary or metamorphic lithology.
5. It is possible to identify lithological boundaries from overall changes in the level of radiation shown on the contoured maps. The degree of this identification can be either obvious or subtle depending on the contrast in the radiometric signature of two adjacent lithologies.

Here followsis a qualitative description of the total and spectral radiometric maps (Figs. 4 to 10). The total-count aeroradiometric map (Fig. 4) shows a wide variation of the measurements from one type of rock to another and to more or less extent between the units of the same rock type [from about 3.0 Ur (over Cretaceous sediments) to 36.7 Ur (over granite rocks of G. Homrat El-Gergab) with an average value of about 12.7 Ur (1.0 Ur = unit of radioelement concentration _ 0.6 R/h _ 1.0 ppm U)]. This wide variation reflects the fact that the mapped area is covered by rocks of various composition. The eU content ranges from 0.9 ppm (over Quaternary sediments) to 10 ppm (over granitic rocks of G. Homrat El-Gergab), with an average value of about 3.0 ppm. The eTh content reaches 40.3 ppm as a maximum value (over granitic rocks of G. Homrat El-Gergab) and diminishes to 3.0 ppm (over Quaternary sediments), with an average value of about 8.9 ppm. The Potassium content ranges from 0.09 % (over Cretaceous sediments) to 3.8 % (over the granitic rocks of G. Dara and G. Homrat El-Gergab), with an average value of about 1.97 %.

The total count radiometric map (Fig. 4) could be divided into four distinct levels of radioactivity, coinciding with the different types of rocks. The first one represents the lowest radioactivity level in the study area (Fig. 4). It is formed of conspicuous elongated zone of parallel repetitive sets trending in NNW and NW directions. Generally, this level decreases in radioactivity from the periphery

towards the center and sometimes with steep radiometric gradients with the higher radioactive levels. The range of radioactivity of this level varies between 2.0 to 7.5 Ur. This level was found to be barren from any radioactive anomalies. It is encountered at ; the northeastern corner (at G. El-Zeit), at the southeastern corner, at the extension of G. Sufr El-Dib (west of Esh El-Mallaha Range) and at the southwestern side of the study area.

The second-intermediate-level ranges in radioactivity from 7.5 to 15.0 Ur (Fig. 4). It is encountered as zones with different shapes distributed all over the study area. This level is not regular and continuous as the first one but possesses gradational contacts with the neighboring and surrounding levels, since it is chiefly interrupted by other radioactivity levels and trending mainly in NNW, NW, NE and ENE directions representing structural fault lines. It shows no evidence for the existence of values of anomalous radioactivity and is associated mainly with Metasediments, Hammamat Sediments, Dokhan Volcanics, Tertiary Sediments and Quaternary Wadi Sediments.

The third - high - level ranges in intensity from 15.0 to 22.5 Ur (Fig. 4). It covers most of the Older and Younger granitic plutons in the study area and is formed of zones of circular to semi-circular and elongated shapes. It is characterized by its high values of aeroradioactivity among the other levels and shows arcuate and sharp contacts with the surrounding levels. It is represented by many localities lying to the northwest of the study area around G. Dara and W. Dara, at G. Homrat El-Gergab (in the southeast of W. Dib within Esh El-Mallaha Range) and to the northwest of W. Dib. The most conspicuous feature of this level is that most of its constituent radiometric closed contours or closures are aligned in a nearly NNW, NW, NE and ENE directions. It is worthy to mention that most of the interpreted radioactive anomalies in the study area are restricted to this high level of radioactivity.

The fourth-very high-level represents the highest radioactivity level within the study area (Fig. 4), which possesses intensity reaching more than 22.5 Ur. It is encountered in the form of masses of nearly circular to oval or elongated shapes, associated with the Younger Granites of G. Dara and G. Homrat El-Gergab, as follows :

1. **Gabal Dara Younger Granites** (at the northwestern corner of the study area) : It is bounded from the east and south by steep radiometric gradients representing structural fault lines trending in NNW and NW directions. The total-count radioactivity ranges from 22.0 to 31.5 Ur, with increasing character towards the center. Most of the radiometric boundaries almost match well with what mapped geologically as Younger Granites. The eU and eTh maps are reflecting the same features and structural indications. The eU content ranges

between 4.0 to 9.6 ppm and the eTh content from 21.0 to 27.4 ppm, while the K- map shows a range from 2.4 to 3.6 K %.

2. **Gabal Homrat El-Gergab YoungerGranites** (at the southeastern side, within Esh El-Mallaha Range) : The very high radioactivity level can be seen over G. Homrat El-Gergab, where it ranges from 22.0 to 36.0 Ur, with increasing character towards the center. Most of the radiometric boundaries almost correspond well with what mapped geologically as Younger Granites. It is also coinciding well with W. Dib structural fault lines trending in NNW and NW directions. The eU, eTh and K maps (Figs. 5, 6 and 7) show the same features and structural indications, where the eU content ranges from 4.0 ppm at the periphery and increases to 9.5 ppm towards the center. The eTh content ranges from 22.5 to 35.5 ppm, while the K- map shows a range between 2.4 and 3.8 K%. This level is considered as representing the radiometric anomalous zones within the area under investigation, which are characterized by their anomalous concentrations of the three radioactive elements. Most of the identified uranium and thorium anomalies lie within this very high level of radioactivity.

On the eU contour map (Fig. 5), there are five levels of eU radiospectrometry; the first-very low-level (< 2.0 ppm) is found mainly over the diorite-epidiorite rocks, metavolcanics and Cretaceous metasediments. The second-low-level (2 to 4 ppm) is recorded over grey granites, metasediments, Hammamat group, Dokhan volcanics, Nubian sandstones and Quaternary sediments, where it occupies the largest part of the study area. The third-intermediate-level (4 to 6 ppm) is located over the grey granites and the younger granites of G. Homrat El-Gergab and the granitic masses around most of the granitic plutons as well as small part of the Quaternary sediments. The fourth- high-level (6 to 8 ppm) is represented by G. Homrat El-Gergab and G. Dara younger granites. The fifth -very high- level (>8 ppm) seems to be associated with younger granites of G. Homrat El-Gergab and G. Dara. The shapes and trends of the contour lines mainly agree well with the shapes and trends of the total-count aeroradiometric map (Fig. 4), especially the NNW, NW, NE and ENE directions. Accordingly, the same structural directions can be traced from this map.

According to the eTh contour map (Fig. 6), it can be divided into four radioactivity levels, the first-low-level (< 4 ppm eTh) is located in the western side of the study area (around Esh El-Mallaha Range and southeast W. Dib), north W. Abu-Had and the northeastern side of the study area and mainly associated with diorite-epidiorite rocks, metasediments and Cretaceous sediments. The second-intermediate-level (4 to 8 ppm eTh) is represented by a large part of the study area and is recorded mainly over the metasediments, Dokhan volcanics, Hammamat sediments, grey granites and Quaternary sediments. The third-high-

level (8 to 16 ppm eTh) is associated with grey and younger granites and Quaternary sediments. It is also recorded over the older granites northwest W. Dib and the younger granites of G. Homrat El-Gergab and G. Dara. The fourth-very high-level (>16 ppm eTh) is associated with the younger granites of G. Homrat El-Gergab and G. Dara. The structural contacts between the radiometric rock units can be traced easily, with their main trends are in the NNW, NW, NE and ENE directions.

On the Potassium (K) contour map (Fig. 7) there are four levels of radioactivity. The first-lowest-level (< 1.4 % K), is located at the northeastern side, around Esh El-Mallaha Range and some parts to the south of W. Dib and the southeastern side in the study area. It is associated with diorite-epidiorite rocks, metavolcanics and Cretaceous sediments. The second- intermediate-level (1.4 - 2.0 % K) is mainly associated with the first one in its localities and is mainly related to metasediments, Dokhan volcanics and Quaternary sediments. The third- high-level (2-2.8 % K) is represented by older and younger granites of G. Homrat El-Gergab, G. Dara and northwest W. Dib. The second and third levels are not so regular and continuous as the first one but possesses gradational contacts with the neighboring and surrounding levels, since it is chiefly interrupted by other aeroradioactivity levels. The fourth -relatively very high - level (> 2.8 % K) is mainly associated with the younger granites of G. Homrat El-Gergab, G. Dara and the sediments which are derived from the younger granite plutons in the study area. The boundaries between the units can be traced easily, especially around the granitic plutons, Cretaceous sediments and Quaternary sediments. The structural trends mainly agree well with the trends discussed earlier in the case of the total-count, eU and eTh maps.

The eU/eTh ratio reaches about 2.3 as a maximum value over the Cretaceous sediments in the extreme west of Esh El-Mallaha Range and diminishes to about 0.05 over the Quaternary sediments to the south of W. Dara in the northern part of the study area (Fig. 8). The average value of eU/eTh ratio attains about 0.5 for the whole area under consideration. This ratio map shows that, there are four prominent anomalous ratios. The first anomalous eU/eTh ratio is located at the extreme southwestern part of Esh El-Mallaha Range, reaching 2.3 in value and is mainly associated with Nubian sandstones. It is characterized by its elongated shape that trends in NNW and NW directions. The second one is located at the extreme northeastern corner, attaining 1.98 in value and is associated with Cretaceous and Tertiary sediments. This anomaly is characterized by its irregular shape and is oriented in nearly NW and NNW directions. The third anomalous eU/eTh ratio lies over G. Monqul younger granites and is characterized by its incomplete form reaching 1.4 in value. The fourth anomalous ratio lies over G.

Abu-Shar younger granites and is characterized by its oval shape reaching 1.7 in value.

The eU/K ratio contour map (Fig. 9) shows four prominent anomalous ratios. The first ratio is located in the southwestern side of Esh El-Mallaha Range and is mainly associated with Cretaceous sediments. It is characterized by an elongated shape oriented in the NNW direction, with a ratio value of about 14.0. The second anomalous ratio is located at the northeastern side of the study area over Cretaceous sediments and is also characterized by an elongated shape, trending mainly in NNW and NW directions with ratio of about 12.6. Two small anomalous ratios could be observed on the contacts between the younger granites and Tertiary sediments in the northern side of the study area around G. Abu-Shar younger granites. These two anomalous ratios are characterized by their oval and elongated shapes which are oriented in nearly NNW and NW directions, with ratio reaching 8.8 in value. Most of the anomalies observed in areas of generally low radiometric response, are false and associated with Cretaceous sediments, with ratio values ranging between 2.0 and 8.0. These false anomalies can help in tracing the contact between Nubian Sandstones and the surrounding rocks. These high values appear to be related to fair increase in eU and eTh measurements with dramatic decrease in the Potassium data reaching to concentrations less than 1.0 %. The prominent high eU/K ratio indicate also that uranium remains relatively immobile in these sediments.

According to the eTh / K ratio contour map (Fig. 10), there is a great similarity between the anomalies of this ratio and the eU / K ones, where there are two prominent anomalies observed in areas of generally high total-count radiometric response. The first anomalous ratio is located in the southeastern side of Esh El-Mallaha Range over G. Homrat El-Gergab younger granites. This anomaly is characterized by its incomplete shape and oriented in the NNW and NE directions with ratio value of 15.5. The second one located nearly at the northeastern part of the study area is mainly associated with Cretaceous sediments. It is characterized by its oval shape and oriented in the NNW and NE directions with ratio value of 14.2. Most of the anomalous ratios are observed in areas of generally low radiometric response. These anomalies are false and associated with Nubian sandstone. They appear to be related to increased thorium and depleted potassium levels in the area of general low radiometric reposes of Quaternary and Cretaceous sediments in which thorium was remained relatively immobile.

QUANTITATIVE INTERPRETATION OF AERORADIO-SPECTROMETRIC DATA

The quantitative interpretation of the gamma-ray spectrometric survey data aims essentially at emphasizing the selection of the real and most promising anomalies for later geophysical, geological and geochemical ground follow-up. In the present work, the quantitative treatment of data obtained from airborne gamma-ray spectrometric survey, is discussed in four ways :

I. Statistical analysis of the aeroradiospectrometric data.

II. Conventional Statistical treatment of the aeroradiospectrometric data.

III. Identification and outlining the aeroradiospectrometric provinces.

IV. Determination of the degree of uranium remobilization.

I. Statistical Analysis of the Aeroradiospectrometric Data

The various aeroradiospectrometric data collected over the study area have been subjected to conventional statistical methods of analysis. These methods include single variate and multivariate analyses. The quantitative interpretation of the Total-Count (T.C.) aeroradiometric survey data of each rock unit was performed to investigate the types of distributions of their data, to establish their characteristic radioactivity statistics and to define the relationships between these units as far as radioactivity is concerned.

The application of these methods facilitated the manipulation of the data and enhanced their interpretation. So, the digital measurements of the different geophysical variables (T.C., eTh, eU and K) were fed into a PC computer. The statistical computations were performed using a software standard package and the statistical treatments of the data were executed as follows :

1. Single Variate Statistical Analysis

Single variate method of analysis is only concerned with analyzing variations in a single random variable. They are generally of quantitative nature and used to describe the statistical characteristics of distributions of the individual geophysical variables according to these 4 steps:

1. Determination and organization of the measured data (T. C. radiometric values) of each rock unit.
2. Mathematical testing of the homogeneity of the data through the application of the chi-square (^{2}) test, which calculates the degree of goodness and fitness

between the normal (theoretical) curve and the observed one at a specific level of confidence (Clark and Cooke, 1988).

3. Calculation of some significant statistics for the distributions under consideration. These include the range (Max. – Min.), the arithmetic mean (X), the standard deviation (S), X+3S, X–3S and the results of ^{2}–test (Table 1).

4. Estimation of the threshold values for the variable that proved to possess normal distributions. These values distinguish an upper anomalous set of data from a lower background set. They were estimated as values lying more than three standard deviations from the arithmetic mean X (Sinclair, 1981).

Table (1) : Summary of Computed T. C. Statistical Characteristics, Single Variate, of the Different Rock Units, Wadi Dib Area, Northern Eastern Desert, Egypt

Ser. No.	Rock unit	No. of Obs.	Range		X (Ur)	S (Ur)	X+3S (Ur)	X-3S (Ur)	^{2}–test Value		Dist. Type
			Min. (Ur)	Max. (Ur)					Calc.	Crit.	
1	WD	2217	6.0	14.1	10.5	1.1	13.8	7.2	51.95	18.31	N. N.
2	TS	399	6.53	13.9	9.9	1.2	13.5	6.3	28.60	15.51	N. N.
3	NSS	1076	3.1	9.4	6.2	0.8	8.6	3.8	37.1	22.36	N. N.
4	YG	1160	8.9	35.9	17.1	2.9	25.8	8.4	29.31	16.92	N. N.
5	HS	230	5.6	12.9	8.6	1.4	12.8	4.4	18.5	12.59	N. N.
6	DV	530	4.8	11.9	8.0	1.3	11.9	4.1	28.8	14.07	N. N.
7	GG	606	7.0	16.8	10.1	2.2	16.7	3.5	32.8	18.31	N. N.
8	DR	107	3.71	9.0	5.9	1.02	8.96	2.84	16.5	11.07	N. N.
9	MV	73	2.9	7.66	4.1	1.13	7.49	0.71	13.42	12.59	N. N.
10	MS	183	3.4	8.4	5.2	0.94	8.02	2.38	14.64	14.07	N. N.

W D : Wadi Deposits (Sediments) T S : Tertiary Sediments

NSS : Nubian Sandstones Y G : Younger Granites

H S : Hammamat Sediments D V : Dokhan Volcanics

G G : Grey Granites D R : Diorite Rocks

M V : Metavolcanics M S : Metasediments

Accordingly, the tested data that show abnormal distributions were subjected to many trials until attaining normal distributions "if possible". This was done either through the exclusion of abnormal (very high and/or very low) measurements or the original rock units that show inhomogeneous distributions could be subdivided into two or more homogeneous subunits. This will be done by the application of multivariate statistical analysis technique.

Finally, according to the compiled geological and the total-count (T.C.) aeroradiometric maps and the application of single variate statistical analysis method, the results of application of the chi-square (^{2}) test shows that all the original rock units on the compiled geological map do not show normal distributions (Table 1). Therefore, these rock units will be treated statistically using multivariate statistical analysis method by applying the Factor Analysis Technique to construct the Interpreted Radiometric Lithologic (IRL) unit map for the study area.

2. Multivariate (Factor) Statistical Analysis

The airborne gamma-ray spectrometric method is a good technique in geological mapping specially in regions where the geology is complex. K^{40}, U^{238} and Th^{232} are usually present in all rocks, but in a wide range of concentrations and relative proportion to each other which help reflect the lithology.

The available data (T. C., eU, eTh and K) are in the form of contoured maps of scale 1:50,000. The study area was digitized along east-west trending profiles on a square grid with 0.5 km spacing and these data were stored in separate files. Three ratios (eU/eTh, eU/K and eTh/K) were calculated from the above data. Again a composite file was prepared to include seven columns [T.C., eU, eTh, K, eU/eTh, eU/K and eTh/K) and 6200 rows (100 x 62) sampled points]. Standard statistics were applied to the data to compute means, measures of dispersion and normality check for each variable. Correlation coefficients among variables were computed as well. A detailed discussion of factor analysis was given Comrey (1973) among others. However, it is a technique by which variables on a set of samples are linearly combined giving rise to new fundamental quantities (factors) which can be named and simply interpreted in the light of sound geologic reasoning.

The present computations were carried out on the Micro-Vax II computer system of the N. M. A. The program extracts the eigen values and eigen vectors from the correlation matrix using the Householder technique by subprogram "tred 2" and matrix inversion by the two subprograms "Ludcmp" and "Lubksp", (Press et al., 1986). Through matrix manipulation, the principal factors were extracted and rotated to a position where each factor would have a large variance of the squared loading and thus the values were maximally spread out. Scores of the original data were calculated, but related to the principal factors. The resultant three factor scores F_1, F_2 and F_3 were subjected to what is simply called clustering. The method consist of considering each data point from factor analysis as a point in X, Y and Z coordinate system where X is F_1, Y is F_2 and Z is F_3.

Now, we are interested in the correlation between all possible pairs of variables in the data matrix. The resultant correlation coefficient matrix between

the seven data (aeroradio- spectrometric) variables of the study area is shown in Table (2), which has seven rows and seven columns. Each entry shows the degree of linear relationship between a pair of variables. So, it gives the view of what the variables share in common with each other. It has been shown that, the matrix is symmetrical; that is, the upper right side is a mirror image of the lower left side and it has values of 1.0 in the diagonal, since the correlation of a variable with itself is equal 1.0. The matrix of correlation coefficients exhibits all the information contained in the original data matrix, concerning the relationships between the variables. It is actually the starting point of factor analysis.

Table (2) : Correlation Coefficient Matrix between the Seven Variables, Wadi Dib area, Northern Eastern Desert, Egypt

Variables	T. C.	eU	eTh	K	eU / eTh	eU / K	eTh / K
T. C., in Ur	1.00	0.82	0.94	0.89	- 0.37	- 0.20	0.33
EU, in ppm	0.82	1.00	0.79	0.57	0.08	0.23	0.48
ETh, in ppm	0.94	0.79	1.00	0.75	- 0.42	- 0.15	0.56
K, in %	0.89	0.57	0.75	1.00	- 0.49	- 0.45	- 0.07
EU / eTh	- 0.37	0.08	- 0.42	- 0.49	1.00	0.85	- 0.01
EU / K	- 0.20	0.23	- 0.15	- 0.45	0.85	1.00	0.42
ETh / K	0.33	0.48	0.56	- 0.07	- 0.01	0.42	1.00

N.B.: Critical Correlation Coefficient (r c) at the 95 % of confidence.

The correlation matrix (Table 2) shows high positive correlations between T.C. and the three variables eU, eTh and K. The relatively strongest positive correlation exists between T. C. and eTh, while the relatively lowest positive correlation lies between eU and eU/eTh ratio. Meanwhile, the negative correlation is distinguished between eU / eTh ratio and T.C., eTh and K as well as between eU/ K ratio and T.C., eTh and K. The relatively highest negative correlation exists between K and eU/eTh ratio, while the relatively lowest negative correlation lies between eU/eTh and eTh/K ratios. Fig. (11-a & b) displays the correlation coefficients of the various four absolute and the three relative aeroradio-spectrometric variables of the study area.

After the correlation matrix has been computed (Table 2), the next step in the factor analysis is to determine how many factor constructs are needed to account for the pattern of values found in correlation matrix. This is done through a process called "factor extraction", which constitutes the second major step in a factor analysis. Instead of discussing the intercorrelation between these variables, factor analysis provides a way of thinking about this interpretationships.

Table (3) : Unrotated Factor Matrix of the data of the Seven Aeroradiospectrometric Variables, Wadi Dib area, Northern Eastern Desert, Egypt.

Factor Variables (F)	F 1	F 2	F 3	F 4	F 5	F 6	F 7
Eigen Values (E.G.)	3.75	2.19	0.85	0.14	0.04	0.02	0.01
E. V. (%)	53.63	31.23	12.16	1.97	0.60	0.26	0.16
Cumulative E.V. (%)	53.63	84.86	97.02	98.99	99.58	99.84	100.0
T. C., in Ur	0.98	0.08	- 0.15	0.05	0.03	0.00	- 0.09
eU, in ppm	0.78	0.52	- 0.22	- 0.26	- 0.08	- 0.01	0.01
eTh, in ppm	0.97	0.16	0.13	0.04	0.11	- 0.07	0.04
K, in %	0.87	- 0.28	- 0.36	0.18	- 0.05	0.05	0.04
eU / eTh	- 0.50	0.73	- 0.45	- 0.02	0.11	0.05	0.01
eU / K	- 0.30	0.93	- 0.10	0.18	- 0.08	- 0.06	- 0.01
eTh / K	0.39	0.65	0.65	0.03	- 0.01	0.07	00.0

The correlation matrix (Table 2) is used to get "unrotated loading matrix" of Table (3), coupled with the extracted Eigen values and their cumulative percent. Factor loadings of variables on each of the unrotated factors are also given. Variation of the Eigen values, their percent as well as their cumulative percent with each of the various seven unrotated factors representing aeroradiospectrometric data of the study area are demonstrated by Fig. (12).

Meanwhile, Fig. (13) shows unrotated factor loadings of the various seven aeroradio-spectrometric variables on each of the first three unrotated factors (F1, F2 and F3). Suffice to say that, the Eigen values are the roots of a series of partial-differential simultaneous equations which display the principal factors in terms of their variance in comparison to the total variance of the original variables, that is, percentages of the contributions of the different factors to the total variance in the multivariate data set.

From Table (3), the first factor variable (T. C.) has an Eigen value of 3.75, where as the other factor variables all have Eigen values less than this value. This means that (T. C.) is, by far, the most important of the seven factor variables for representing the variation in the measurements. Besides, eU and eTh have Eigen values equal 2.19 and 0.85 respectively, which are substantially larger than the last four factor variables. So, perhaps the first three factor variables should all be considered. Therefore, it can be seen that, although the process of factor extraction began with seven factor variables, the total variations of the sample points could be explained by means of the first three variables or factors and thus work could be executed only in 3-dimensional space rather than 7-dimensional space. The highest factor variable in the sense that the weight of factor loading is largest is recorded

in the first column (53.63). The sequent factor variables become progressively smaller (31.23 and 12.16) respectively.

The 7-dimensional factor space can be reduced without significant loss of information into 3-dimension of space (principal factors). These three factors are quite interpretable and represent 97.02 % of the total system information, which is sufficient to interpret the available data, where the first three factor variables are loaded by 53.63, 31.23 and 12.16 % of the data respectively.

Table (4) shows the three principal factors (F1, F2 and F3) extracted from the previous Table (3). They were rotated using varimax method. Fig. (14) shows the varimax rotated factor loadings of the various seven aeroradiospectrometric variables on each of the first three rotated factors (F1, F2 and F3) of the study area.

Table (4) : Loadings of Factors (Varimax Rotated), Wadi Dib area, Northern Eastern Desert, Egypt.

Factor Variables (F)	F1	F2	F3
T. C., in Ur	0.961	- 0.200	0.162
eU, in ppm	0.881	0.269	0.280
eTh, in ppm	0.858	- 0.242	0.429
K, in %	0.879	- 0.372	- 0.220
eU / eTh	- 0.164	0.972	- 0.112
eU / K	- 0.082	0.918	0.327
eTh / K	0.209	0.132	0.966

It can be concluded from Table (4) that the first factor (F1) has appreciably high positive loadings with four variables (T.C., eU, eTh and K). This allows saying that this factor is primarily composed of only four variables. This factor can thus be interpreted according to the lithological significance of those variables. This reflects the presence of these three radioactive elements in the host acidic rocks. F1 exhibits inverse loadings with eU/eTh and eU/K as negative values and is weakly loaded with eTh / K. Therefore, F1 can be identified as the factor of "integrated radioactivity".

The second factor (F2) is highly and positively loaded with eU/eTh and eU/K and weakly loaded with eU and eTh / K. F2 is also inversely loaded with T. C., eTh and K. Therefore, F2 refers to rocks which have low alkalinity.

The third factor (F3) is highly loaded with eTh / K and weakly loaded with T.C., eU, eTh and eU/K. F3 is also inversely loaded with K and eU / eTh. Therefore, F3 explains the sites of alteration or mineralization inside the rock units. It can be called that "intra-rock unit differentiation" factor.

The standard scores of the three factors (F1, F2 and F3) are multiplied by 100 before contouring on separate maps (Figs. 15, 16 and 17). These factor scores characterizing different rock units in the study area, are best summarized in Table (5). These units are named in the light of the published geological map (Fig. 5).

It was clearly found that (F1) positive scores, (Fig. 15) outline highly radioactive rocks as younger and older granites (YG-1, YG-2, YG-3, YG-4, GG-1 & GG-2) of the study area. The positive scores also outline Wadi sediments (WD-2) in the extreme north of Esh El-Mallaha Range at the southeastern corner of the study area and Tertiary sediments (TS-1), west of G. Homrat El-Gergab granites. Meanwhile, the negative scores of (F1) outline the Dokhan Volcanics (DV-1 and DV-2), Wadi sediments (WD-1), Diorite-Epidiorite rocks (DR), Tertiary sediments (TS-2), Hammamat Sediments (HS-2), Metasediments (MS) and Cretaceous Nubian Sandstones (NSS-1 and NSS-2).

The second factor (F2) positive scores, (Fig. 16) outline the Cretaceous Nubian Sandstones (NSS-1 & NSS-2), two types of granitic rocks (YG-1 & YG-2) and Hammamat Sediments (HS-1). On the other hand, the negative scores of this factor outline Wadi Sediments (WD-3) and Metavolcanics (MV).

The third factor (F3) positive scores, (Fig. 17) outline the two types of younger granitic rocks (YG-1and YG-2), Cretaceous Nubian Sandstones (NSS-2) and Tertiary Sediments (TS-2). Meanwhile, the negative scores of (F3) outline the older granitoids (GG-1 and GG-2).

The results obtained through the application of factor analysis technique made it possible to emphasize most of the geologic units, delineate new geologic units and correct some rock types on the geologic map of the study area -as far as radiospectrometry is concerned-via the statisticaltreatment of the aeroradio-spectrometric measurements registered over the different Interpreted Radiospectro-metric Lithologic (IRL) units of the study area.

The outcome interpreted rock unit map (Fig. 18) reflects a similar content of radioelements and probably, common features that could be found in the lithologic composition for each of the interpreted units. Besides, it reflects also a similarity in the geochemical behavior of the various aeroradiospectrometric statistics of each rock unit. The first factor (F1) could be called the factor of "integrated radioactivity" and it outlines rocks of appreciable radioactivity, while the other two factors (F2 and F3) could be named the factors of the intra-rock unit differentiation. Consequently, it was possible to delineate twenty Interpreted Radiospectrometric Lithologic (IRL) units as a result of matching the three factor score maps (Figs. 15, 16 and 17) with the geologic map (Fig. 3).

The interpreted rock unit map (Fig. 18) could be traced, which shows that the Wadi sediments were represented as one unit on the geologic map, could be divided into three IRL units (WD-1, WD-2 and WD-3). Tertiary Sediments were divided into two IRL units (TS-1 and TS-2) and the Cretaceous Nubian Sandstones were divided into two IRL units (NSS-1 and NSS-2). Younger granitic rocks which were represented as one unit on the geologic map, could be divided into four IRL units (YG-1, YG-2, YG-3 and YG-4). The boundaries of these units are defined clearly by positive contours of the first factor (F1) and the differentiation between these IRL units were controlled by the values of these contour lines and on the basis of factor score maps. The Hammamat Sediments were divided into two IRL units (HS-1 and HS-2) and Dokhan Volcanics were divided into two IRL units (DV-1 and DV-2) on the interpreted rock unit map (Fig. 18). The majority of older granitoid IRL units have been easily distinguished and sharply separated at the zero contour from the surrounding rock units. The older granitoid IRL unit which is located in the southwestern and central parts of Esh El-Mallaha Range was divided into two IRL units (GG-1 and GG-2). These IRL units are defined clearly by the negative contour lines of the third factor (F3). Diorite-Epidiorite rocks, Metavolcanics and Metasediments were represented on the interpreted rock unit map (Fig. 18) as DR, MV and MS respectively.

Table (5) : Factor Scores Characterizing Different IRL Units, Wadi Dib area, Northern Eastern Desert, Egypt.

F1			F2			F3		
From	**To**	**IRL Unit**	**From**	**To**	**IRL Unit**	**From**	**To**	**IRL Unit**
80	260	YG-3 & YG-4	0	1070	NSS-1	0	260	YG-2
150	550	YG-1	0	800	NSS-2	0	300	NSS-2
200	470	YG-2	0	80	YG-1	0	350	TS-2
0	100	WD-2	0	130	HS-1	0	600	YG-1
0	140	TS-1	0	160	YG-2	- 180	- 50	GG-1
0	180	GG-2	- 110	0	WD-3	- 220	- 50	GG-2
0	300	GG-1	- 210	-100	MV			
- 80	0	WD-1						
-120	0	DV-1						
- 150	0	DR						
- 190	0	DV-2						
- 210	0	TS-2						
- 230	0	HS-2						
- 260	0	MS						
- 290	0	NSS-1 & NSS-2						

II. Conventional Statistical Treatment of Aeroradiospectrometric Data

Conventional statistical computations were conducted on the original aeroradiospectro-metric survey data without employing any type of transformation. This is in accordance with the work of Sarma and Kock (1980) who recommended the performance of statistical computations on the original data. A variable possesses a coefficient of variability (CV % = S/X * 100), where (S) is the standard deviation and (X) is the arithmetic mean.

In order to carry out the techniques of statistical analysis on the airborne gamma-ray spectrometric data, digitized profiles along traverse lines were collected for each IRL unit. To check the normality of each rock unit, the coefficient of variability (CV %) is examined, if (CV %) of a certain unit is less than 100 %, the unit exhibits normal distribution. The computed arithmetic means (X) and standard deviations (S) of the total-count radioactivity (T.C.) and the concentrations of the absolute potassium (K, in %), equivalent Uranium (eU, in ppm) and equivalent Thorium (eTh, in ppm) for all the Interpreted Radiometric Lithologic (IRL) units in the study area are given and summarized in Tables (6 to 9). In addition, their computed coefficients of variability (CV %) and the significant factors (X + 2S & X - 2S) and (X + 3S & X - 3S) for each (IRL) unit are also indicated in the same tables.

Table (6) : Results of the Computed T. C. Characteristic Statistics of the Various IRL units, Wadi Dib area, Northern Eastern Desert, Egypt.

IRL Unit (Fig. 18)	No. of Obs	X (Ur)	S (Ur)	CV %	Range		X+2S (Ur)	X+3S (Ur)	X-2S (Ur)	X-3S (Ur)	χ^2 – test Value		Dis. Type
					Min (Ur)	Max (Ur)					Calc.	Crit.	
WD-1	961	9.31	0.58	6.23	6.7	12.6	10.47	11.05	8.15	7.57	13.53	19.68	N
WD-2	717	11.9	0.63	5.29	8.4	14.3	13.16	13.79	10.64	10.01	3.20	9.49	N
WD-3	539	12.6	0.94	7.45	9.8	16.5	14.49	15.43	10.73	9.79	6.76	15.51	N
TS-1	116	12.1	1.31	10.82	8.3	16.2	14.72	16.03	9.48	8.17	10.87	15.51	N
TS-2	283	9.81	1.13	11.52	5.6	13.4	12.07	13.2	7.55	6.42	5.50	15.51	N
NSS-1	416	7.11	1.01	14.2	3.9	11.2	9.13	10.14	5.09	4.08	6.28	15.51	N
NSS-2	660	6.17	1.35	21.88	3.4	10.9	8.87	10.22	3.47	2.12	9.70	14.07	N
YG-1	162	21.6	3.42	15.82	10.5	36.4	28.46	31.88	14.78	11.36	4.91	14.07	N
YG-2	246	19.8	2.39	12.05	9.4	29.6	24.61	27.00	15.05	12.66	5.14	14.07	N
YG-3	340	17.3	2.93	16.96	8.9	27.7	23.13	26.06	11.41	8.48	9.64	11.07	N
YG-4	443	13.1	2.10	16.02	6.8	20.3	17.31	19.41	8.91	6.81	7.29	14.07	N
HS-1	90	10.1	0.91	8.97	6.3	13.1	11.96	12.87	8.32	7.41	4.21	9.49	N
HS-2	140	8.21	0.73	8.89	5.1	10.7	9.67	10.40	6.75	6.02	7.67	14.07	N
DV-1	316	9.97	1.09	10.93	6.8	14.1	12.15	13.24	7.79	6.70	8.50	12.59	N
DV-2	215	7.65	0.58	7.58	3.1	9.96	8.81	9.39	6.49	5.91	7.15	14.07	N
GG-1	409	11.1	0.89	8.05	7.11	14.9	12.83	13.72	9.27	8.38	13.07	15.51	N
GG-2	195	8.19	1.21	14.77	7.4	12.6	10.61	11.82	5.77	4.56	8.86	11.07	N
DR	95	6.31	0.69	10.94	3.71	9.3	7.69	8.38	4.93	4.24	6.24	11.07	N
MV	61	4.13	1.23	29.78	2.5	8.11	6.59	7.82	1.67	0.44	4.36	9.49	N
MS	160	5.03	0.88	17.49	3.41	8.27	6.79	7.67	3.27	2.39	11.6	16.92	N

N : Normal Distribution at the 95 % level of confidence

Table (7) : Results of the Computed eU Characteristic Statistics of the Various IRL units, Wadi Dib area, Northern Eastern Desert, Egypt.

IRL Unit (Fig. 18)	No. of Obs.	X (ppm)	S (ppm)	CV %	Range		X+2S (ppm)	X+3S (ppm)	X-2S (ppm)	X-3S (ppm)	χ^2 test Value		Dis. Type
					Min. (ppm)	Max. (ppm)					Calc.	Crit.	
WD-1	961	1.34	0.46	34.32	1.10	3.20	2.26	2.72	0.42	0.04	11.17	14.07	N
WD-2	717	1.78	0.51	28.65	1.20	3.90	2.80	3.31	0.76	0.25	6.90	15.51	N
WD-3	539	2.50	0.74	29.60	1.96	4.88	3.98	4.72	1.02	0.28	4.41	15.51	N
TS-1	116	2.74	0.36	13.14	1.80	4.10	3.46	3.82	2.02	1.66	3.45	12.59	N
TS-2	283	2.11	0.53	25.12	1.40	3.90	3.17	3.70	1.05	0.52	4.11	12.59	N
NSS-1	416	2.32	0.39	16.80	0.96	4.30	3.10	3.49	1.54	1.15	9.12	14.07	N
NSS-2	660	1.91	0.43	22.51	0.93	4.00	2.77	3.20	1.05	0.62	9.10	16.92	N
YG-1	162	3.94	0.81	20.56	3.60	9.20	5.56	6.37	2.32	1.51	11.4	16.92	N
YG-2	246	3.32	0.41	12.35	2.30	7.10	4.14	4.55	2.50	2.09	7.11	14.07	N
YG-3	340	2.52	0.49	19.44	2.10	4.90	3.50	3.99	1.54	1.05	12.3	16.92	N
YG-4	443	1.95	0.54	27.69	1.40	4.00	3.03	3.57	0.87	0.33	2.11	7.81	N
HS-1	90	2.30	0.52	22.61	1.30	3.90	3.34	3.86	1.26	0.74	10.5	14.07	N
HS2	140	1.68	o.32	19.05	1.10	3.00	2.32	2.64	1.04	0.72	10.2	16.92	N
DV-1	316	2.19	0.45	20.55	0.95	3.70	3.09	3.54	1.29	0.84	8.71	12.59	N
DV-2	215	1.54	0.38	24.67	0.91	2.90	2.30	2.68	0.78	0.40	6.01	16.92	N
GG-1	409	2.96	0.51	17.23	1.50	6.30	3.98	4.49	1.94	1.43	6.74	14.07	N
GG-2	195	1.66	0.40	24.10	1.20	3.30	2.46	2.86	0.86	0.46	3.82	11.07	N
D R	95	1.34	0.44	32.83	0.93	2.70	2.22	2.66	0.46	0.02	4.71	12.59	N
MV	61	1.29	0.42	32.56	0.90	2.60	2.13	2.55	0.45	0.03	7.27	11.07	N
M S	160	1.46	0.33	22.60	0.92	2.88	2.12	2.45	0.80	0.47	9.12	14.07	N

Since the computed mean values of the measured airborne radiospectrometric variables (T.C., K, eU and eTh) are not of the same order of magnitude; it becomes very difficult to compare the scattering of the obtained data for each variable relative to the others through the computed standard deviation values.

Table (8): Results of the Computed eTh Characteristic Statistics of the Various IRL units, Wadi Dib area, Northern Eastern Desert, Egypt

IRL Unit (Fig. 18)	No. of Obs.	X, ppm	S, ppm	C V %	Range		X+2S (ppm)	X+3S (ppm)	X-2S (ppm)	X-3S (ppm)	2_{-} test Value		Dis. Type
					Min. (ppm)	Max. (ppm)					Calc	Crit.	
WD-1	961	5.40	0.90	16.67	3.30	9.10	7.20	8.10	3.60	2.70	10.6	15.51	N
WD-2	717	6.44	0.70	10.86	4.10	10.4	7.84	8.54	5.04	4.34	3.69	14.07	N
WD-3	539	8.21	0.63	7.67	4.90	11.6	9.47	10.1	6.95	6.32	4.01	14.07	N
TS-1	116	7.33	0.57	7.78	4.80	10.1	8.47	9.04	6.19	5.62	3.31	11.07	N
TS-2	283	4.98	0.73	14.66	3.20	8.90	6.44	7.17	3.52	2.79	3.42	11.07	N
NSS-1	416	5.20	1.10	21.15	3.10	9.00	7.40	8.50	3.00	1.90	9.81	15.51	N
NSS-2	660	3.89	0.83	21.34	3.20	7.10	5.55	6.38	2.23	1.40	8.47	14.07	N
YG-1	162	17.5	2.32	13.23	10.3	38.1	22.2	24.5	12.9	10.6	7.62	14.07	N
YG-2	246	14.2	1.31	9.23	9.90	30.4	16.8	18.1	11.6	10.3	6.39	12.59	N
YG-3	340	10.4	1.39	13.37	5.10	22.6	13.2	14.6	7.62	6.23	3.61	12.59	N
YG-4	443	8.93	1.36	15.23	4.40	16.3	11.7	13.0	6.21	4.85	5.83	15.51	N
HS-1	90	6.67	0.99	14.84	5.10	10.2	8.65	9.64	4.69	3.70	1.35	14.07	N
HS-2	140	4.71	0.69	14.65	2.80	9.30	6.09	6.78	3.33	2.64	5.41	11.07	N
DV-1	316	6.8	0.67	9.85	3.20	10.2	8.14	8.81	5.46	4.79	3.51	14.07	N
DV-2	215	4.77	0.75	15.72	3.10	8.30	6.27	7.02	3.27	2.52	5.22	18.31	N
GG-1	409	8.69	1.21	13.92	4.10	14.3	11.1	12.3	6.27	5.06	3.43	14.07	N
GG-2	195	6.02	0.79	13.12	3.40	9.90	7.60	8.39	4.44	3.65	8.74	12.59	N
DR	95	4.10	0.31	7.56	3.10	5.40	4.72	5.03	3.48	3.17	9.42	15.51	N
MV	61	4.21	0.78	18.53	3.10	6.70	5.77	6.55	2.65	1.87	2.10	11.07	N
MS	160	5.12	1.00	19.53	3.50	9.20	7.12	8.12	3.12	2.12	7.51	14.07	N

Table (9) : Results of the Computed K Characteristic Statistics of the Various IRL units, Wadi Dib area, Northern Eastern Desert, Egypt

IRL Unit (Fig. 18)	No. of Obs	X (%)	S (%)	C V %	Range		X+2S (%)	X+3S (%)	X-2S (%)	X-3S (%)	2_{-} test Value		Dis. Type
					Min. (%)	Max. (%)					Calc.	Crit.	
WD-1	961	0.96	0.19	19.79	0.90	1.60	1.34	1.53	0.58	0.39	2.10	3.84	N
WD-2	717	1.27	0.22	17.32	0.97	2.00	1.71	1.93	0.83	0.61	3.61	7.81	N
WD-3	539	2.00	0.32	16.00	1.21	2.98	2.64	2.96	1.36	1.04	6.93	9.49	N
TS-1	116	1.00	0.15	15.00	0.92	1.63	1.30	1.45	0.70	0.55	7.67	11.07	N
TS-2	283	0.97	0.13	14.29	0.90	1.48	1.17	1.30	0.65	0.52	4.66	12.59	N
NSS-1	416	1.12	0.14	12.50	1.00	1.60	1.40	1.54	0.84	0.70	9.11	15.51	N
NSS-2	660	0.97	0.10	10.31	0.91	1.31	1.17	1.27	0.77	0.67	5.64	18.31	N
YG-1	162	2.32	0.31	13.36	1.70	3.80	2.94	3.25	1.70	1.39	2.21	9.49	N
YG-2	246	2.00	0.24	12.00	1.40	3.00	2.48	2.72	1.52	1.28	3.47	9.49	N
YG-3	340	1.64	0.18	10.97	1.20	2.50	2.00	2.18	1.28	1.10	2.13	7.81	N
YG-4	443	1.11	0.27	24.32	0.99	2.00	1.65	1.92	0.57	0.30	2.79	7.81	N
HS-1	90	1.24	0.28	22.58	0.98	2.20	1.80	2.08	0.68	0.40	9.37	12.59	N
HS-2	140	0.94	0.27	28.72	0.90	1.76	1.48	1.75	0.40	0.13	3.59	9.49	N
DV-1	316	1.22	0.29	23.77	0.96	2.10	1.80	2.09	0.64	0.35	4.76	7.81	N
DV-2	215	0.95	0.13	13.68	0.90	1.40	1.21	1.34	0.69	0.56	2.74	9.49	N
GG-1	409	1.47	0.33	22.45	1.01	2.71	2.13	2.46	0.81	0.48	4.01	11.07	N
GG-2	195	0.98	0.17	17.35	0.93	1.70	1.32	1.49	0.64	0.47	4.28	9.49	N
DR	95	0.94	0.11	11.7	0.90	1.30	1.16	1.27	0.72	0.61	8.46	14.07	N
MV	61	0.96	0.16	16.67	0.91	1.47	1.28	1.44	0.64	0.48	2.89	9.49	N
MS	160	1.18	0.21	17.79	0.93	1.94	1.60	1.81	0.76	0.55	6.78	11.07	N

Accordingly, the values of coefficients of variability (C V %) of these four variables were calculated to perform such comparison within the various IRL units. Inspection of these computed coefficients of variability showed that they may provide quantitative measures regarding the degree of homogeneity of the distributions. The higher the coefficient of variability, the lower is the degree of homogeneity (Abdel Nabi, 1990).

The relatively lower values of C V % of the total-count radioactivity in relation to potassium, equivalent uranium and equivalent thorium in all IRL units (Tables 6 to 9) reflect the high degree of homogeneity in the distributions of the total radioactivity. It is believed that the observed tendency of K ; which is a major element in the rock-forming minerals; towards the homogeneity can be explained as that K has relatively high geochemical stability under the oxidizing and hydrothermal conditions. In comparison with the eU and eTh, the observed relative tendency-of these two trace elements-toward nonhomogeneity is mainly attributed to the similarity in their geochemical characteristics and their relatively higher mobility under the same conditions. The higher values of C V % of eU and eTh reflect the presence of considerable variations with respect to their distributions within the IRL units which, consequently, indicate relatively low degree of homogeneity.

In addition, an exact numerical test, the Chi-square (^{2}) test, was also applied to check the normality of the distributions of aeroradiospectrometric measurements. This important test was applied, at the 95% level of confidence, to the T. C. and the absolute radioelement concentration measurements. The results of application of the ^{2}-test revealed that they are normally distributed in all the IRL units that were delineated through the use of factor analysis technique, since the calculated values of the Chi-square are less than the critical ones (Tables 10 to 13). This reflects the radiometric uniformity of the IRL units which indicates the homogeneity in their rock composition. So, the authors would like to draw the attention to the accuracy of the factor analysis technique in the lithological mapping.

It was observed that the minimum aeroradiospectrometric computed statistics are those associated with the Diorite-Epidiorite Rocks and Metavolcanics, while the intermediate values are belonging to the Hammamat sediments and Cretaceous Nubian Sandstones. Meanwhile, the maximum values are connected with the granites.

III. Identification and Outlining the Radiospectrometric Anom-alous Zones

In order to identify and outline a significant individual uranium and/or thorium anomaly, it is important to examine the gamma-ray spectrometric data of each IRL unit. It was important, first of all, to examine the average background

values for each rock type and delineate the areas having values equal to or exceeding the calculated arithmetic means plus multiples two or three standard deviations.

The statistical treatment of uranium and/or thorium data in terms of individual younger and older granitic units provides means of searching for areas with anomalously high uranium and / or thorium content within each IRL unit. To recognize the possible uranium and /or thorium deposits from gamma-ray survey data, it is very important to examine also the ratios of the different three radioelement concentrations, which are considered good indicators for identifying the uranium and / or thorium enrichment over the other two radioelements.

In a similar manner, the increase or the high-recorded values in the total-count data greatly aids in uranium and / or thorium anomaly identification. Fig. (19) shows fourteen uranium, thorium as well as mixed uranium and thorium anomalies, which were identified in the area under investigation.

The second step of defining significant uranium and / or thorium anomalies is by examining the composite stacked profiles for regions of high eU, eTh and their ratio values indicating uranium and / or thorium enrichment over the other two natural radioelements. Ratio measurements are particularly useful in airborne gamma-ray spectrometry, because they are less affected by source geometry and surface variability than are individual element data and hence, are better indicators of preferential accumulation of radioelements. Accordingly, inspection of the ratio data greatly aids in uranium and / or thorium anomaly identifications.

In the present work, the individual uranium and / or thorium anomalies, interpreted in this survey area, are based on the investigation of the composite aeroradiospectrometric stacked profile data and searching for areas where one of the two radioelements has been concentrated preferentially over the other two radioelements. This is highly supported by a similar increase in the ratios of this radioelement over the other two. In a similar manner, the increase or the high recorded values in the total-count data greatly aids in uranium and / or thorium anomaly identification.

Consequently and depending upon the previous statements, fourteen aeroradiospectro-metric anomalies were delineated, three mixed uranium & thorium, six uranium and five thorium anomalies were identified in the study area. The locations of these identified anomalies are shown on the interpreted aerial radiospectrometric anomaly map (Fig. 19) of the area under consideration.

A set of composite aerial radiospectrometric stacked profiles have been constructed for the identified uranium and thorium anomalies (Figs. 20 and 21) in order to facilitate the follow up of the response of one and the same anomaly on the

different aeroradiospectrometric channels. These profiles have been traced out from the flight lines and the Aero-Service sheets on which the final corrected aerial gamma-ray radiospectrometric survey data are presented in profile form, plotted at a horizontal scale of 1 : 50,000. Displayed on these profiles are the total-count (T. C., in Ur), the three radioelements in standard concentration units : potassium (K, in %), equivalent uranium (eU, in ppm) and equivalent thorium (eTh, in ppm), in addition to their three ratios (eU / eTh, eU / K and eTh / K).

Through the examination of the composite stacked profiles of the outlined (Fig. 20), three mixed uranium & thorium anomalies have shown that the eU, eTh, K and T. C. channels exhibit significant increases over the background levels.

On the other hand, the preferential enrichment of Uranium and Thorium can be seen in the relatively high response of the eU/eTh, eU/K and eTh/K traces. By the same way, examination of the data of composite spectrometric profiles of the identified six Uranium anomalies (Figs. 20 and 21) has been shown that the eU and T. C. channels exhibit considerable increase over the background levels, while K and eTh channels show low responses. On the other hand, the preferential enrichment of Uranium can be seen in the relatively high response of the eU / eTh and eU / K traces.

Meanwhile, the examination of the data of composite spectrometric profiles of the identified five Thorium anomalies (Fig. 21) shows clearly that each of them exhibits a relatively high eTh concentration associated with a corresponding high response for the eTh/K ratio and at the same time a considerable increase in the T. C. rate with a relatively flat response for the eU/eTh ratio. This points out to the fact that Thorium has been preferentially enriched over the other two radioelements (U and K).

Table (10) : Maximum Amplitudes (Absolute and Ratio) of the Airborne Radiospectrometric (U, Th and mixed U+Th) anomalies as well as their Geologic Environment, Wadi Dib area, Northern Eastern Desert, Egypt.

Anomaly No. (Figs. 20 & 21)	Maximum Amplitude							Geologic Environment
	T. C. (Ur)	K (%)	eU (ppm)	eTh (ppm)	eU / eTh	eU / K	eTh / K	
(U+Th) -1	22.32	1.67	9.83	19.84	5.21	26.31	8.19	G. Dara Younger Granites
(U+Th) -2	29.41	3.34	9.90	18.32	1.56	7.89	8.74	G. Homrat El-Gergab Younger Granites
(U+Th) -3	20.13	2.54	8.23	13.14	1.14	5.26	5.12	North G. Homrat El-GergabYounger Gr.
U – 1	19.82	0.90	8.93	7.11	1.47	15.33	11.02	Southeast G. Dara Younger Granites
U – 2	19.12	1.03	8.81	5.38	2.87	16.32	8.38	South G. Monqol Older Granites
U – 3	25.96	1.43	9.32	8.66	1.89	15.73	10.21	North W. Dib Older Granites
U – 4	15.22	0.89	7.67	5.14	2.47	18.41	9.72	Northwest W. Dib Older Granites
U – 5	27.87	1.49	9.53	9.21	1.87	6.98	7.53	North G. Abu Shar Younger Granites
U – 6	20.95	1.13	7.58	6.13	2.23	16.71	12.34	G. Abu Shar Younger Granites
Th – 1	29.97	3.81	7.47	18.22	1.20	3.91	11.36	South W. Dara Younger Granites
Th – 2	15.10	2.21	6.38	17.83	0.81	4.65	7.31	Northwest G. Tarbul Younger Granites
Th – 3	26.62	2.34	6.38	18.13	0.92	5.01	9.32	North G. Tarbul Younger Granites
Th – 4	24.6	2.53	6.20	17.47	0.72	3.94	8.62	Metasediments, Esh El-Mallaha Range
Th – 5	16.22	1.74	4.87	18.10	0.94	5.24	15.63	Older Granites, Esh El-Mallaha Range

Table (10) summarizes the maximum measured values of the various radiospectrometric Variables (T. C., K, eU, eTh, eU / eTh, eU / K and eTh / K) ; in standard concentration units ; for the interpreted eU and eTh anomalies, in addition to their geologic associations.

The authors would like to direct attention to this importance of these Mixed Uranium + Thorium, Uranium and Thorium anomalies.

The third step of defining significant uranium and / or thorium anomalies could be attained through the calculation of the average uranium, thorium, potassium and eTh / eU ratio values for each of the various rock units of the study area and comparing them with the crustal average values for each rock type. This correlation is indicated in Table (11), which shows that the average values of K and eU in the different rock units in the study area are less than their equivalent values in the crustal rocks, except in the intermediate igneous rocks which have average values almost equivalent to those of the crustal rocks. The eTh average and the range of values in the different rock units are also less than those in the equivalent crustal rocks except in cases of the averages of YG-1, YG-2 and YG-3 (acidic igneous rocks), where the range is relatively higher than their equivalent values in the crustal rocks.

Table (11): Correlation between the Radioelement Concentrations for Crustal Rocks (IAEA, 1979 and Boyle, 1982) and Different Rock Units of Wadi Dib area, Northern Eastern Desert, Egypt.

Rock Types		K (%)	U or eU (ppm)		Th or eTh (ppm)		Th/U or eTh/eU	
		Average	Average	Range	Average	Range	Average	Range
Acidic Igneous	**Crustal Average**	4.00	4.50	1 -12	18	5 –20	4	2 – 10
	YG - 1	2.32	3.94	3.6-9.2	17.53	10.3-38.1	3.94	3.1-7.2
	YG - 2	2.00	3.32	2.3-7.1	14.20	9.9-30.4	3.37	2.4-5.9
	YG - 3	1.64	2.52	2.1-4.9	10.40	5.1-22.6	3.12	1.9-6.2
	YG - 4	1.11	1.95	1.4-4.0	8.93	4.4-16.3	2.82	1.6-4.1
Intermediate Igneous	**Crustal Average**	1.50	2.30	0.5-7.0	9.00	2.00-20	4	2.0-6.0
	GG - 1	1.47	2.96	1.5-6.3	8.69	4.1-14.3	3.9	2.8-6.8
	GG - 2	0.98	1.66	1.2-3.3	6.02	3.4-9.9	3.4	1.6-6.1
Sediments	**Crustal Average**	2.00	2.50	o.7-7.5	9.50	2.0-26	3.5	1 – 12
	NSS - 1	1.12	2.32	0.96-4.3	5.20	3.1-9.0	2.1	0.7-7.9
	NSS - 2	0.97	1.91	0.93-4.0	3.89	3.2-7.1	3.2	0.6-6.8
	TS - 1	1.00	2.74	1.8-4.1	7.33	4.8-10.1	3.39	1.3-8.3
	TS - 2	0.97	2.11	1.4-3.9	4.98	3.2-8.9	2.98	1.9-5.2
	WD - 1	0.96	1.34	1.1-3.2	5.40	3.3-9.1	3.36	1.1-6.2
	WD - 2	1.27	1.78	1.2-3.9	6.44	4.1-10.4	2.77	1.2-4.6
	WD - 3	2.00	2.50	1.96-4.88	8.21	4.9-11.6	3.4	1.4-5.4

These differences, either lower or higher, may be due to the presence of some basic or acidic dykes, which contain lower or higher concentrations of radioactive minerals intruded in these rocks. Besides, the values indicated in this research work are based on aerial survey and not on ground survey.

The average values of eTh / eU ratio in the study area is higher than their average ratio values in the equivalent crustal rocks. This may be due to increased uranium content in some units or lower thorium content in most units in the study area, except in the ranges of intermediate igneous rocks which have range values lower than those in the equivalent crustal rocks. This may be due to the intrusion of some basic or acidic dykes in these rocks or the result of the presence of some structural lines, such as faults, which may involve lower or higher concentrations of radioelements.

From the foregoing correlation, it could be concluded generally that all types of rocks which prevail in the study area have average values either lower than, almost equal to or within the crustal averages.

IV. Determination of Uranium Remobilization Degree

There are two stages of uranium mobilization that could take place during metamorphism. The first stage of uranium mobilization is oxygen-bearing atmosphere factor for uranium ore formation as well as for fundamental and local uranium source formation. Oxygen-bearing ground waters are effective uranium mobilizing agents, which can leach uranium dispersed in rocks and uranium can later be concentrated within sediments. The second stage of uranium mobilization could take place during the metamorphism of these sediments and later on through magma generation from the metamorphosed sediments. These geological processes assist the multifold mobilization of uranium, formation of its fundamental and local sources and the first economic concentration of uranium. (Simov, 1988).

Heier (1965) considered the regional metamorphism acts as a potentially-active process of element fractionation involving migration of the elements. He observed that much of the uranium and thorium in rocks appear to be in leachable positions, possibly adsorbed on mineral surfaces rather than in distinct mineral lattice positions. So, uranium and thorium would, therefore, be more easily affected by metamorphic processes.

Much of the mineralized areas can indicate that uranium tends to increase erratically with increasing potassium. This reflects the greater mobility and, therefore, the impermanence of uranium under hydrothermal and supergene conditions.

Uranium having two valency states is most susceptible to transportation under later hydrothermal conditions and / or weathering processes especially under hot-humid conditions and be precipitated away from thorium and potassium.

The uranium is one of the first elements to become remobilized during metamorphism (Heier, 1965). That is due to the fact that uranium can easily form the soluble uranyl ion (UO_2^{++}), particularly in hexavalent state and

consequently it becomes very mobile. Uranium may be transported under late-stage hydrothermal conditions and be precipitated away from thorium and potassium (IAEA, 1988).

The variations of uranium and thorium with their ratios in each rock unit can be interpreted as follows:

1. If U/Th ratio increases strongly with uranium but not with thorium, post-magmatic remobilization and redistribution of uranium is suggested and this could be a favorable economic criterion, because uranium might have been concentrated into deposits within or near the granites.
2. If U/ Th ratio tends to increase somewhat with uranium concentration and is independent on the thorium concentration, limited redistribution after intrusive event occur either because there was no percolation of fluids to mobilize uranium or because the bulk of uranium is located within stable accessory minerals.
3. If U/Th ratio is inversely correlated with thorium and varies directly with uranium, the radioelement distribution is at least in part governed by magmatic processes and the thorium was fixed in the early stage of magmatic evolution.

The correlation between uranium and thorium with their ratios within the younger and older granitic plutons are graphically represented in (Fig. 22) as follows :

The bulk of Homrat El-Gergab younger Granites (YG-1, Fig. 22) is characterized by a strong direct relation between eU and eTh. The eU/eTh ratio tends to increase or varies directly with eU concentration and inversely with eTh. This suggests that thorium was fixed in the early stages of magmatic evolution, i.e., thorium remained relatively immobile in the original rock or the rock is melted and thorium was concentrated mainly in the primitive phases of magmatic evolution and is, therefore, present in lesser concentrations in the more differentiated phases.

In the case of the granitic rocks of Gabal Dara (YG-2, Fig. 22), the eU / eTh ratio increases strongly with eU concentration and inversely with eTh concentration, while the eU concentration shows nearly no change with eTh concentration. Such relations indicate that there has been strong remobilization, i.e., post magmatic redistribution of uranium (Charbonneau, 1982).

It can be seen from the younger granites (YG-3 and YG-4, Fig. 22) that the radioelement distribution of these granitic units is at least governed by magmatic processes, where eU/eTh ratio varies directly with uranium concentration and inversely with thorium concentration. Meanwhile, eU varies directly eTh.

In case of the older granitic rocks of GG-1 and GG-2 (Fig. 22), the eU / eTh ratio varies directly with uranium and inversely with thorium. These relations reflect that thorium has remained relatively immobile in the older granites.

Generally, the inverse correlation between eU / eTh ratio and eTh concentration in the younger and older granites in the study area, indicate that radioelement distribution were at least partly governed by magmatic processes.

SUMMARY AND CONCLUSIONS

The main purpose of this study is to delineate and map the primary lithological units using the aeroradiospectrometric survey data as the main source of information. Besides, the significant radiospectrometric anomalies were outlined by searching for areas of anomalously high concentrations of uranium and / or thorium, which could be favourable sites for potential radioactive mineral deposits.

The main results and conclusions achieved through the present study from the airborne gamma-ray spectrometric survey of the area under investigation corroborated with the available geological information could be summarized in the following :

1. The aeroradioactivity measurements recorded over the study area vary widely from one type or rock to another and to more or less extent between the units of the same rock type. This wide variation (from 3.3 to 36.7 Ur) reflects the fact that the area is covered by rocks of various composition. Generally, the younger granitic rocks (especially of G. Homrat El-Gergab and G. Dara) possess and manifest the highest radioelement concentrations in the study area. Meanwhile, the lowest concentrations are restricted to the metavolcanics. The intermediate radioelement concentration level is mainly associated with metasediments, Dokhan volcanics, Hammamat sediments and Nubian sandstones.

2. The analysis of the gamma-ray spectrometric data shows a general relationship to the principal rock units and structural trends. However, they provide information about the faulted and fractured zones of highest average radioactivity levels. The qualitative and quantitative interpretation of the aeroradiospec-trometric survey data show a great similarity between the T. C. map and the three radioelement maps (K, eU and eTh) concerning the general features, gradient of the contours and the distribution of the anomalies and their trends.

3. The gamma-ray spectrometric maps show that, the total - count radioactivity reaches about 36.7 Ur as a maximum value over the younger granitic rocks of G. Homrat El-Gergab and G. Dara and 3.3 Ur as a minimum value over the metavolcanics and Cretaceous sediments, with an average value of about

12.7 Ur for the whole study area. Equivalent uranium (eU) concentration ranges from 0.9 ppm (over Quaternary sediments) to 10 ppm (over younger granitic rocks of G. Homrat El-Gergab and G. Dara). Meanwhile, the average abundance of eU reaches about 3.0 ppm for the whole study area. Equivalent thorium (eTh) concentration reaches 40.3 ppm as a maximum value (over the younger granitic rocks of G. Homrat El-Gergab and G.. Dara) and diminishes to 3.0 ppm (over Quaternary sediments). The average abundance of eTh in the study area attains about 8.9 ppm. Potassium (K) content ranges from 0.09 % (over Cretaceous sediments) to 3.8 % (over the younger granitic rocks of G. Dara and G. Homrat El-Gergab). The average abundance of potassium in the study area reaches about - 1.97 %.

4. The most prominent structural features that could be drawn from the aeroradiospectrometric variable maps (T. C., K, eU and eTh) are the major fault lines that run in the NW, NNW, NE and ENE directions. Such interpreted aeroradiospectrometric structural lines could be correlated well with the fault systems shown on the compiled geological map of the study area.

5. Strong eU/eTh and eU/K anomalies were observed over fault zones and contacts between the granites and Quaternary sediments.

6. The aerospectrometric data have been statistically analyzed and correlated with the available compiled geological map of thestudy area, which resulted in the delineation of several new geologic units and some structures with surface expressions. The multivariate (Factor) statistical analysis technique was used as a base for such study, especially as a tool for surface geologic mapping to delineate the different rock units from the radiospectrometric point of view. This technique was applied to the aeroradiospectrometric data to help in performing a coordinate transformation from the radioelement concentrations and their ratios to a system of three independent coordinates. The values of the factor loadings were found by the process of factor analysis and the standard scores were used. The analysis begins with a matrix of correlation coefficients between data variables to deduce to what extent these variables are related. The analysis also includes the calculation of the standard statistics as the arithmetic mean, standard deviation and normality check for each variable in all units. In general, factor analysis is a technique by which variables measured over a set of samples are linearly combined giving rise to a new fundamental quantities (factors), which can be named factor scores. The calculated factor scores (F1, F2 and F3), which reflect the interrelationship of the seven radiospectrometric variables (T.C., K, eU, eTh, eU/eTh, eU/K and eTh/K), are used for directly differentiating and outlining the different rock units in W. Dib area, Northern Eastern Desert, Egypt. The first Factor (F1) was called the factor of "integrated radiospectrometry" and it clearly outlines rocks of

appreciable radioactivity. Meanwhile, the second and third factors (F2 and F3) are the factors of "intra-rock unit differentiation". Consequently, it was possible to delineate twenty interpreted radiospectro-metric lithologic (IRL) units, as a result of matching the three factor score maps with the primary geological map. Thus, mapping factor scores is a powerful tool for differentiating rock units on score maps. The interpreted rock unit map reflects a similar content of radioelements and probably common features could be found in the lithologic composition for each of the IRL units. It reflects also a similarity in the geochemical behaviour of the various aeroradiospectrometric parameters of each rock unit. The identity and contacts of some mapped rock exposures or units were ascertained through this work, while others were modified, subdivided or corrected partially on the basis of their radioelement content.

7. The computed descriptive statistical characteristics of the aeroradiospectrometric data were calculated for all the IRL units in the study area. The arithmetic mean (X), standard deviation (S), coefficient of variability (CV %) and the two (upper and lower) significant thresholds (X 2S and X 3S) for the four radiospectrometric variables (T.C., K, eU and eTh) of each IRL unit were computed. It was observed that there is a wide range of radioactivity among the various IRL units and exposures in the study area. Characteristic high mean aeroradioactivity values are connected with the granitic rocks. Meanwhile, low mean values are correlated with metavolcanics and diorite-epidiorite rocks. In addition, the chi-square(^{2}) test was applied to check the normality of the distribution of aeroradio- activity measurements, which revealed that the T. C. radioactivity, concentrations of the three radioelements (K, eU and eTh) are normally distributed for all the IRL units, which reflects uniform units of homogeneous rock composition.

8. The defining of significant radioactive anomalies has been performed by three ways. The first way stands on the basis of exceeding two or three standard deviations from the arithmetic mean for each radiospectrometric variable (X + 2S or X + 3S) in each IRL unit. The second way of defining significant radioactive anomalies is executed by examining the stacked profiles for regions of high eU, eU / eTh and eU / K values. The third way is carried out by correlating the eU, eTh and K concentrations in crustal rocks (Boyle, 1982) and the computed equivalent concentrations in the study area. This correlation shows that generally, all types of rocks that prevailed in the study area have average values either lower or within the crustal average. The study revealed the presence of fourteen relatively moderate aeroradiospectrometric anomalies : three mixed uranium & thorium, six uranium and five thorium. However, for many reasons, these anomalies can't be counted as of no significance and

ignored, but ground follow-up investigations are warranted over all the interpreted anomalies. It was evident throughout this work that, most of the identified anomalies are confined to topographic highs. This may indicate real radioelement enrichment and hence should be considered as promising targets for further detailed ground follow-up geological, geophysical and geochemical studies in the field as well as collecting representative samples for laboratory analyses. The spatial distribution of the outlined radiospectrometric anomalies was found to be closely related to the surface faulting system prevailing in the study area. The NW, NNW, NE and ENE-striking faults proved to have significant impacts on the localization of the majority of these anomalies. This may attract the attention to a potential and structurally-controlled uranium and/or thorium mineralization, since such faults can act as channel ways for the mineralizing solutions.

9. The variations of uranium and thorium with their ratios reflect the amount of remobili- zation of uranium and showed that high remobilization is indicated in some types of granites (YG-2). This means that post magmatic redistribution of uranium took place.

10. From the point of view of radioelement exploration, it is recommended that the NNW, NW and NE structures could be of prime importance and are considered as significant targets for follow-up and ground (Field) investigations.

REFERENCES

Abdel Nabi, S.H. (1990) : Geophysical investigation of aerospectrometric and aeromagnetic anomalies in the vicinity of Gabal Idid El-Gedan area, Eastern Desert, Egypt. Ph. D. Thesis, Faculty of Science, Ain Shams University, Cairo, Egypt, 159 p.

Aero-Service (1984) : Final operational report of airborne magnetic /radiation survey in the Eastern Desert, Egypt, for the Egyptian General Petroleum Corporation, Cairo, Egypt. Aero Service, Houston, Texas, U. S. A., April, 1984, Six Volumes.

Boyle, R. W. (1982) : Geochemical prospecting for thorium and uranium deposits :Elsevier, Amsterdam and New York, 498 p.

Charbonneau, B. W. (1982) : Radiometric study of three radioactive granites in the Canadian Shield : Elliot Lake, Ontario, Fort Smith ; and Fury and Hecla, N. W. T. In uranium in granites, Ed. by Maurice, Y.T., Geological Survey of Canada, Paper 81-23, pp. 91-99.

Clark, G. M. and Cooke, D. (1988) : "A basic course in statistics". English Language Book Society / Edward Arnold Publishers) Ltd., London.

Comrey, A. L. (1973) : A first course in factor analysis. Academic Press, New York, 1 6 p.

Conoco Coral Corporation (1988) : Geological map of Egypt, scale 1 : 500,000 – NG 36 NE Qusseir. The Egyptian General Petroleum Corporation, 1 map.

El-Gaby, S., List, F.K. and Tehrani, R. (1988) : Geology, evaluation and metallogenesis of the Pan-African Belt in Egypt, in the Pan-African Belt of Northeast Africa and adjacent areas. Ed. by S. El-Gaby and R.O. Greilling, pp. 17 - 68, Friedr. Vieweg, Braunschweig, Federal Republic of Germany.

El-Gaby, S., List, F. K. and Tehreni, R. (1990) : The basement complex of the Eastern Desert and Sinai : In the Geology of Egypt. Ed. By Said, R., Published by Balkema, A. A., Rotterdam, Netherlands, pp. 175 - 181.

El-Kholy, D. M. (1995) : Geology and Radioactivity of Esh El-Mallaha Range with Emphasis on the Granite of Gabal Homrat El-Gergab area, Northern Eastern Desert, Egypt. Ph. D. Thesis, Cairo University, Giza, Egypt, 207 p. (Unpubl.).

El-Shazly, E. M. (1977) : The geology of the Egyptian region. In the Ocean Basins and Margins. Ed. By Nairn, A. E. M., Kanes, W. H.and Stehli, F.G., Plenum Publishing Corporation, pp.379-444.

Egyptian Geological Survey & Mining Authority (1978) : Geological map of the Qena Quadrangle, Scale 1 : 500 000, Geological Survey, Cairo, Egypt. 1 map.

Francis, M. H. (1972) : Geology of the basement rocks in the North Eastern Desert between Latitudes 27 30 and 28 00 N. Annals of the Geological Survey of Egypt.V. 2, pp.161-180.

Harman, H. H. (1960) : Modern factor analysis. University of Chicago, USA.

Hassan, M. A. and Hashad, A. H. (1990) : Precambrian of Egypt. In the Geology of Egypt. Ed. By Said, R., Published by Balkema, A. A., Rotterdam, Netherlands, pp.201-245.

Heier, K. S. (1965) : Metamorphism and chemical differentiation of the crust. Geologiska Foreningens Stockholm Forhandlingar, V. 87, pp. 249 - 256.

International Atomic Energy Agency (1979) : Gamma-ray surveys in uranium exploration. Technical Report Series, No. 186, Vienna, Austria, 90 p.

International Atomic Energy Agency (1988) : Geochemical Exploration for uranium. Technical Report series, No. 284, Vienna, Austria, 97 p.

Press, W. H., Flannery, B. P., Teukolsky, S. A. and Vetterling, W. T. (1986) : Numerical Recipes, the art of scientific computing. Cambridge University Press, 817 p.

Riad, A. M., El-Sayed, A., Ahmed, A. M. and Abdalla, A. H. (1978) : Results of prospecting for rare metals, Non-Ferrous metals and gold in the area of Wadi Dara, El-Urf, El-Mallaha, Abu Marwa, Hammad and Bali in 1976-1977. Internal Report, The Egyptian Geological Survey and Mining Authority. No. 3 / 1978, 131p.

Sarma, D. D. and Koch, G. S. (1980) : A statistical analysis of exploration geochemical data for uranium. Mathematical Geology, V. 12, No. 2, pp. 99 - 114.

Saunders, D. F. and Potts, M. J. (1976) : Interpretation and application of high-sensitivity airborne gamma-ray spectro-meter data. IAEA. Symposium on exploration for uranium ore deposits, Vienna, Austria, pp. 107 - 124, IAEA-SM 208 / 45.

Simov, S. D. (1988) : Formation of uranium deposits. International Atomic Energy Agency (IAEA) - TC 450. 5 / 14, Vienna, Austria.

Sinclair, A. H. (1981) : Application of probability graphs in mineral exploration special Volume No. 4, Vancouver, B. C. Canada.

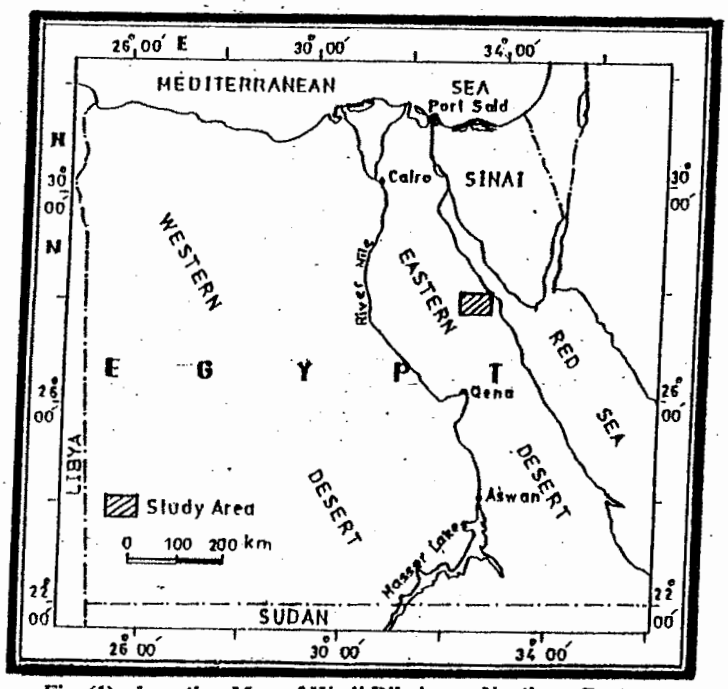

Fig. (1) : Location Map of Wadi Dib Area, Northern Eastern Desert, Egypt

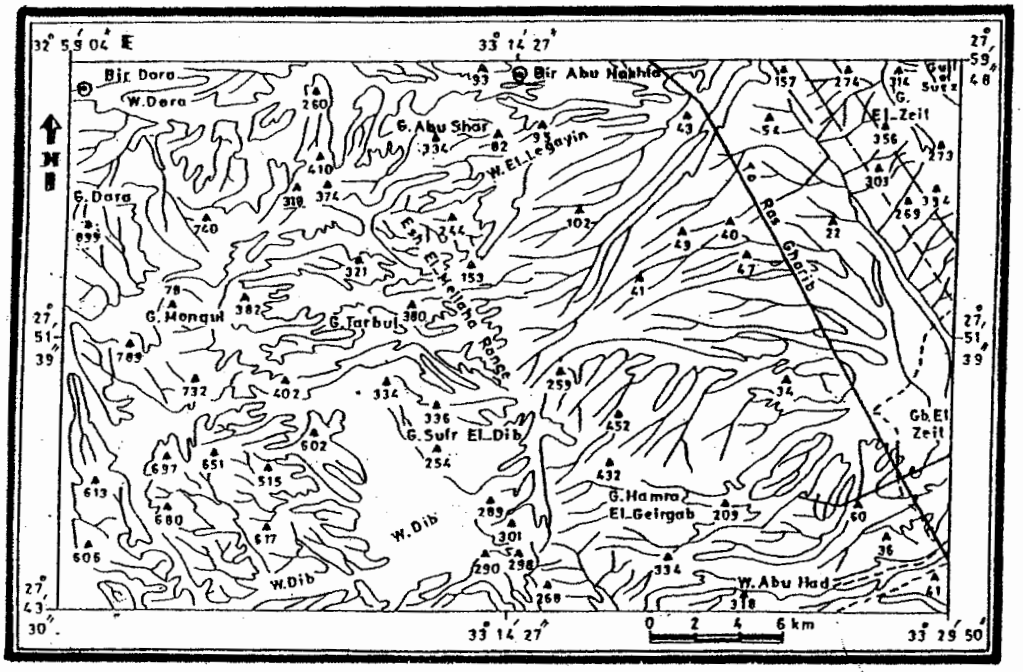

Fig. (2) : Topographic Map of Wadi Dib Area, Northern Eastern Desert, Egypt

LEGEND

▲ 259 : Triangulation Point in m ⊙ : Well (Bir)

G. : Gabal (Mountain) W. (Wadi)

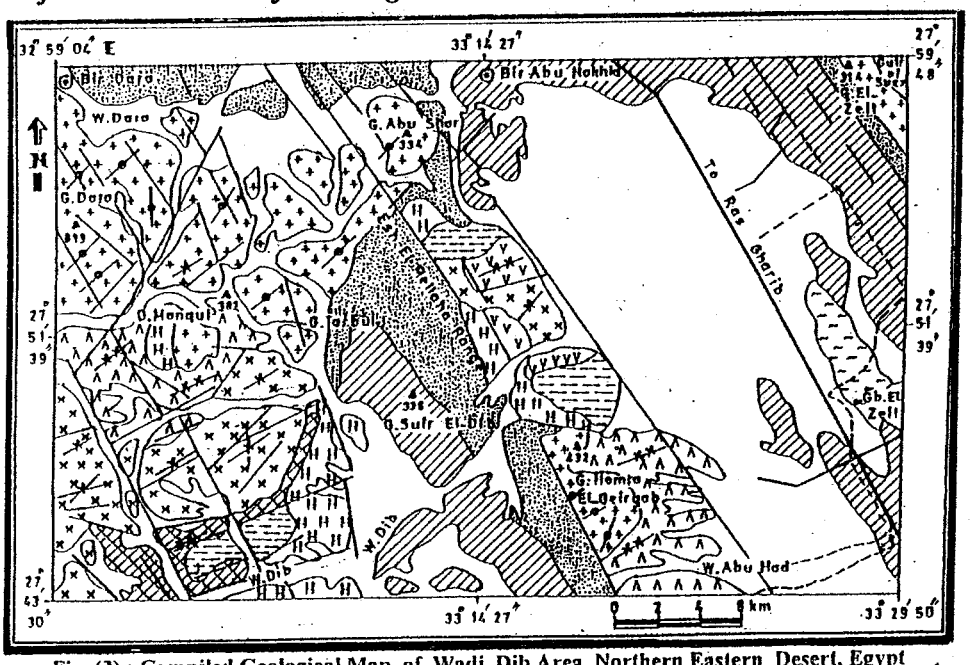

Fig. (3) : Compiled Geological Map of Wadi Dib Area, Northern Eastern Desert, Egypt
(after M. H. Francis, 1972, Geological Survey of Egypt, 1978 and Conoco Coral Corporation, 1988)

LEGEND

: Quaternary (Wadi Sediments)
: Nubian Sandstones
: Hammamat Sediments
: Diorite-Epidiorite Rocks
: Major Faults
: Wadi (Dry Valleys)
: Major Faults (Inferred) / Track of Secondary Road
: Sabkha Sediments
: Post-Granite Dykes
: Dokhan Volcanics
: Metavolcanics
: Main Roads
G. : Gabal (Mountain)
: Tertiary Sediments
: Younger Granitoids
: Older Granitoids
: Metasediments
: Geologic Boundaries
: Wells (Birs)

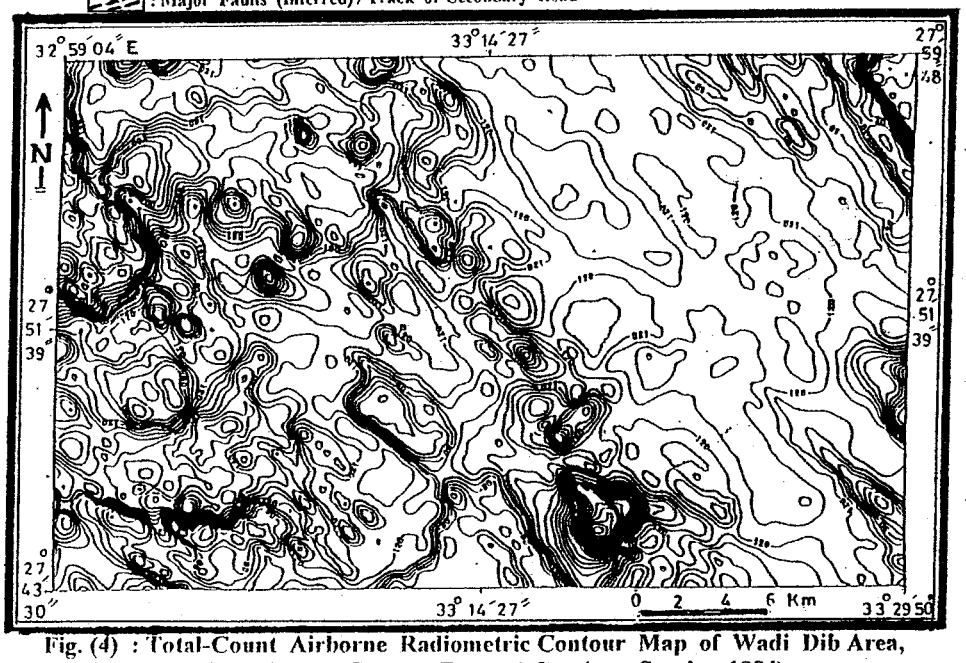

Fig. (4) : Total-Count Airborne Radiometric Contour Map of Wadi Dib Area, Northern Eastern Desert, Egypt (after Aero-Service, 1984)

LEGEND

H : T. C. Aeroradiometric Highs
L : T. C. Aeroradiometric Lows
Contour Interval = 1.0 Ur
Map Values in units of one tenth of 1 Ur

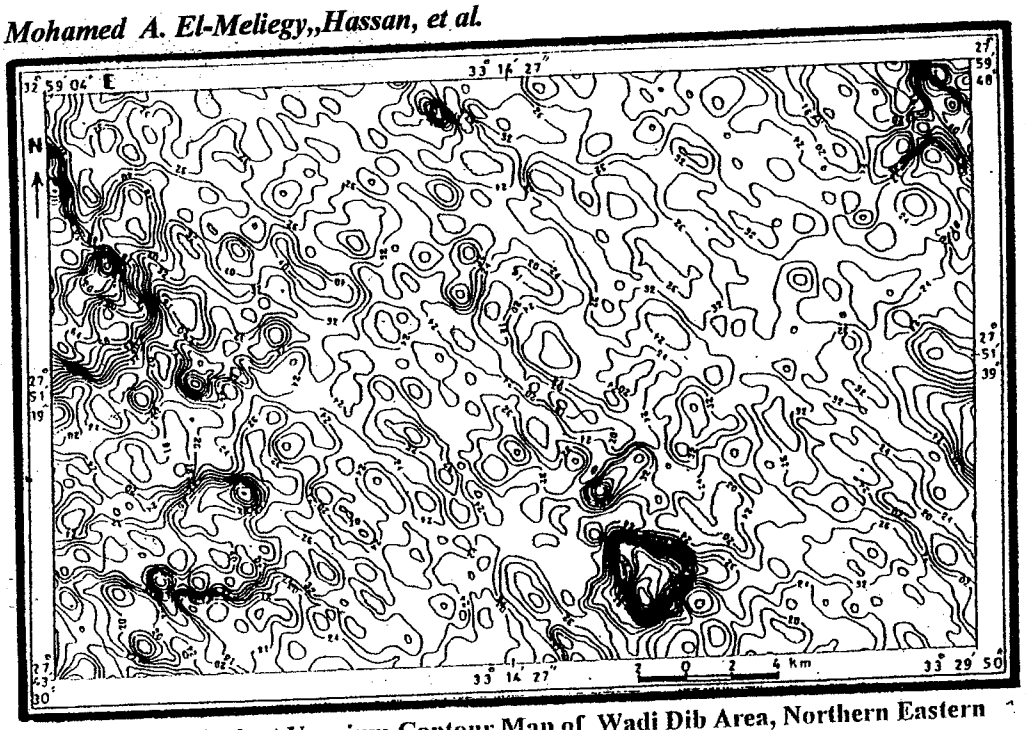

Fig. (5) : Equivalent Uranium Contour Map of Wadi Dib Area, Northern Eastern Desert, Egypt (after Aero-Service, 1984)

LEGEND

(H) : eU Highs
(L) : eU Lows

Contour Interval = 0.4 %
Map Values in units of one tenth of 1 ppm eU

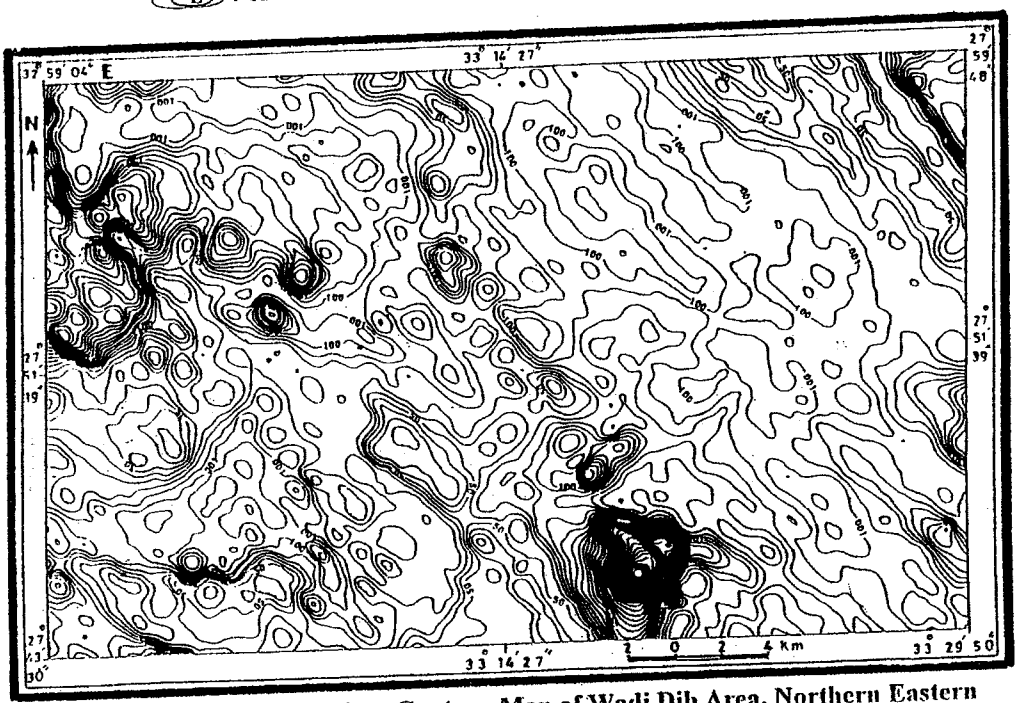

Fig. (6) : Equivalent Thorium Contour Map of Wadi Dib Area, Northern Eastern Desert, Egypt (after Aero-Service, 1984)

LEGEND

(H) : eTh Highs
(L) : eTh Lows

Contour Interval = 1.0 ppm
Map Values in units of one tenth of 1 ppm eTh

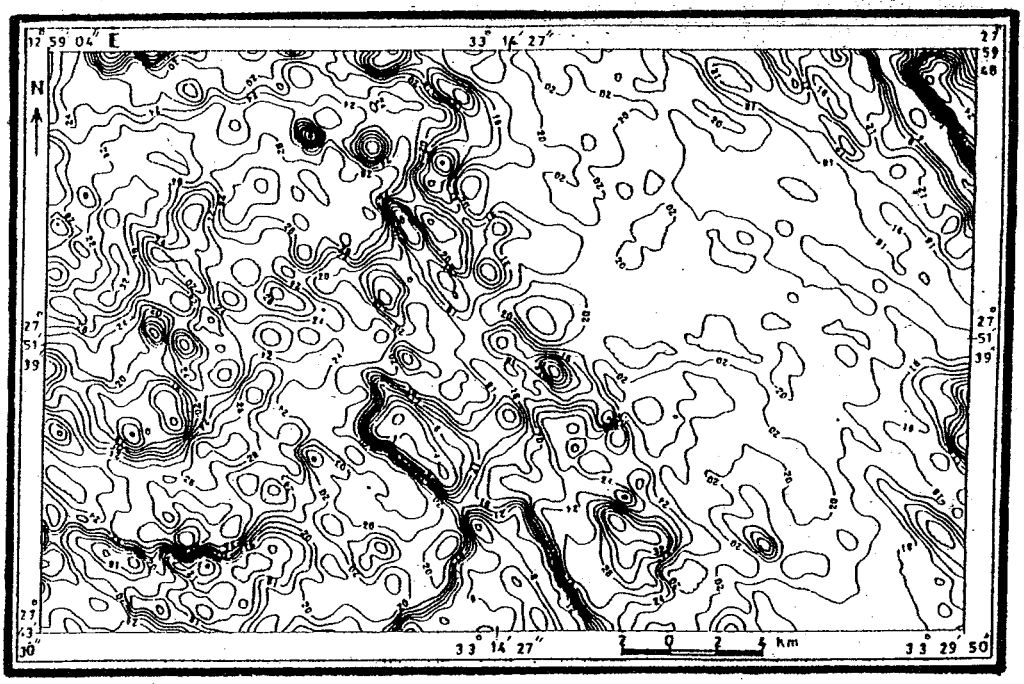

Fig. (7) : Potassium Contour Map of Wadi Dib Area, Northern Eastern Desert, Egypt (after Aero-Service. 1984)

LEGEND

H : K Highs — Contour Interval = 0.2 %

L : K Lows — Map Values in units of one tenth of 1% K

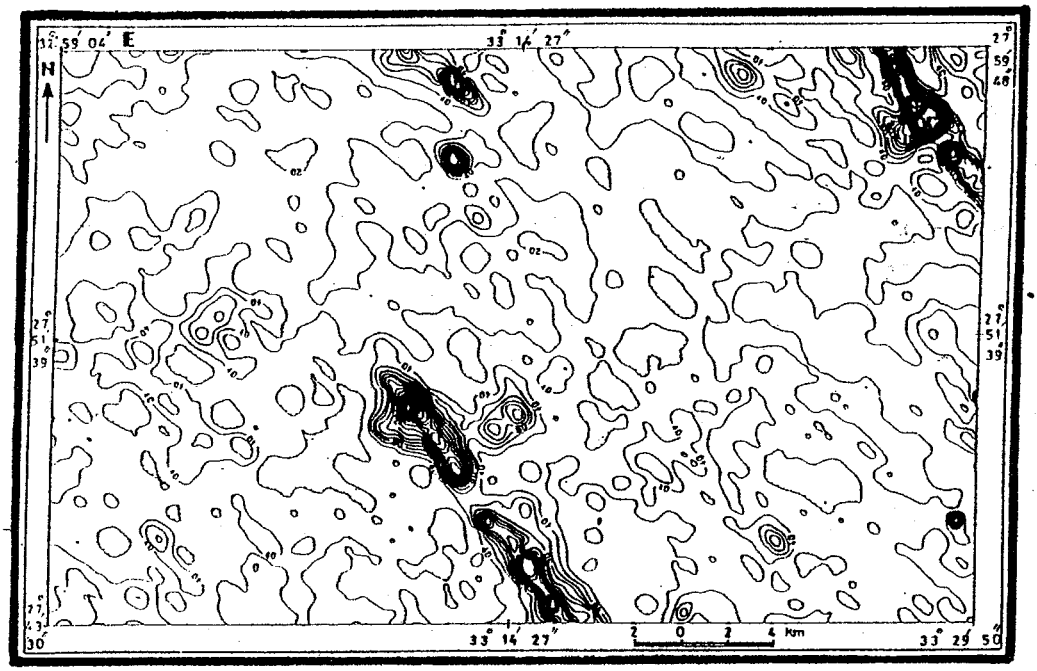

Fig. (8) : Equivalent Uranium / Equivalent Thorium Ratio Contour Map of Wadi Dib area, Northern Eastern Desert, Egypt (after Aero-Service, 1984)

LEGEND

H : eU / eTh Highs — Contour Interval = 0.2

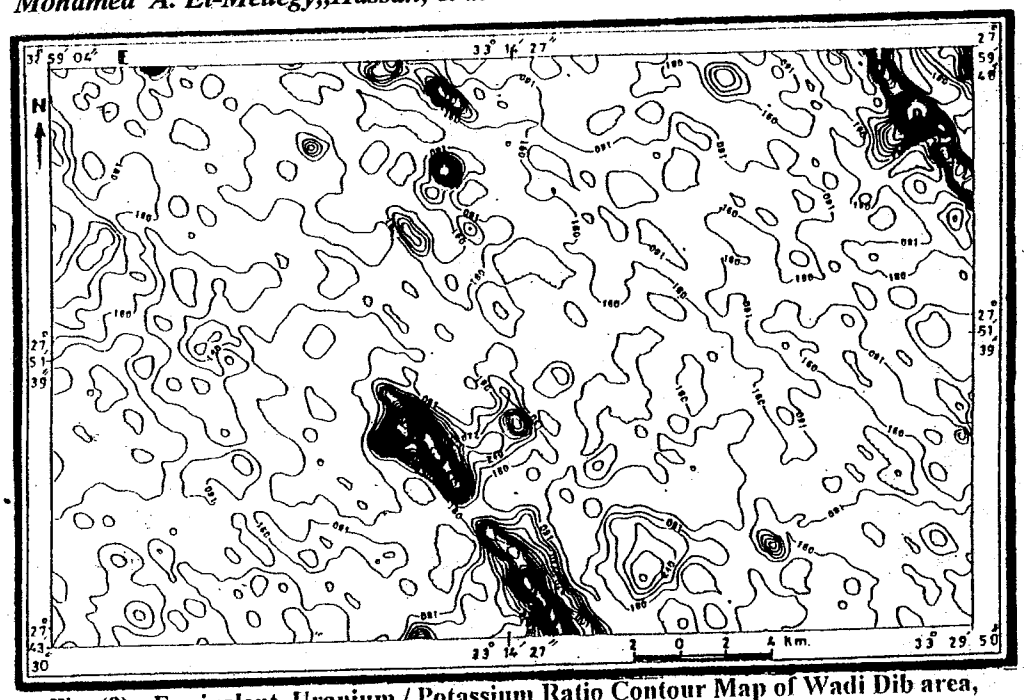

Fig. (9) : Equivalent Uranium / Potassium Ratio Contour Map of Wadi Dib area, Northern Eastern Desert, Egypt (after Aero-Service, 1984)

LEGEND

(H): eU / K Highs
(L): eU / K Lows
Contour Interval = 0.4
Map Values in units of one hundredth of eU / K

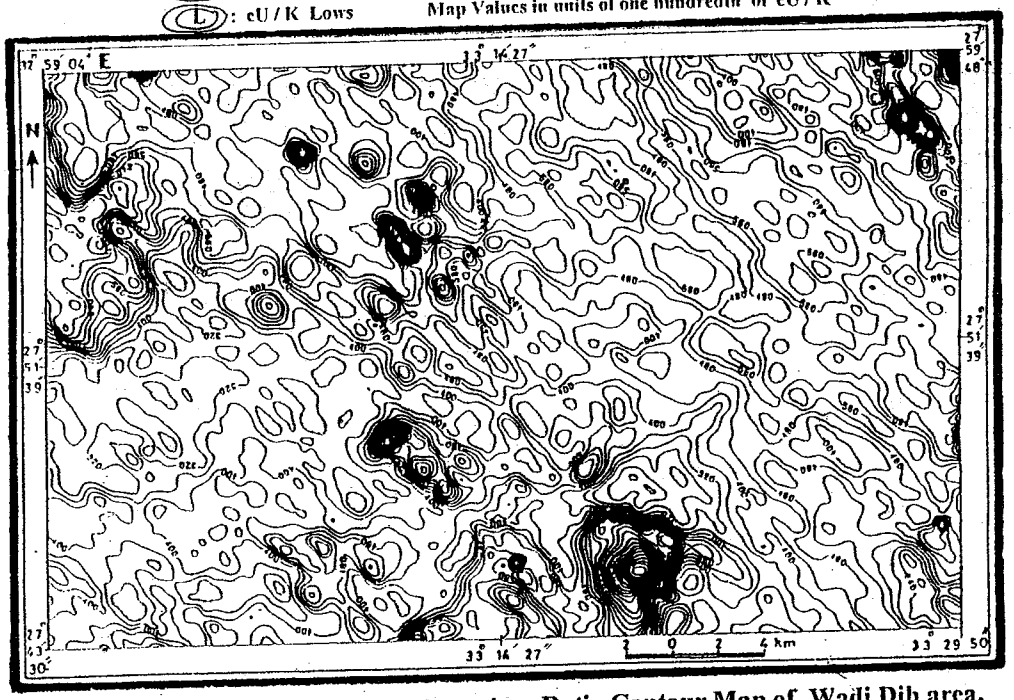

Fig. (10) : Equivalent Thorium / Potassium Ratio Contour Map of Wadi Dib area, Northern Eastern Desert, Egypt (after Aero-Service, 1984)

LEGEND

(H): eTh / K Highs
(L): eTh / K Lows
Contour Interval = 0.1
Map Values in units of one hundredth of eTh / K

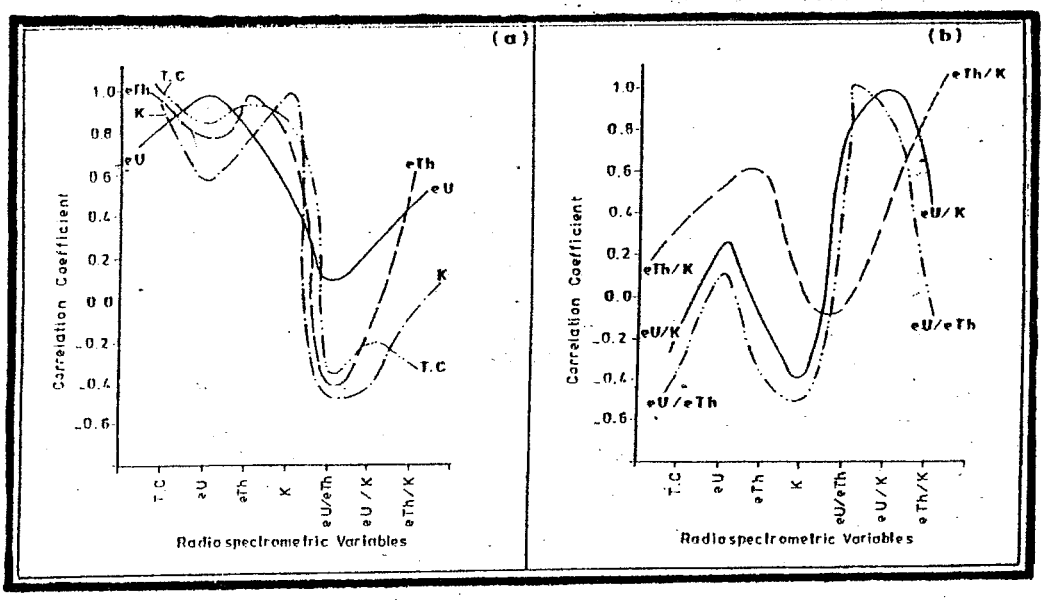

Fig. (11) : Correlation Coefficients (Table 2) of the Various (a) Four Absolute- and (b) Three Relative-Aerial Radiospectrometric Variables, Wadi Dib area, Northern Eastern Desert, Egypt

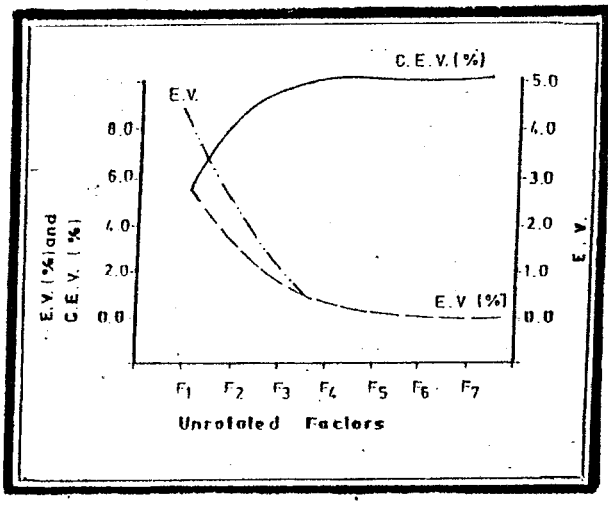

Fig. (12) : Variation of the Eigen Values (E. V.), their Percent (E. V., %) as well as their Cumulative Percent (C. E. V., %) with each of the various Seven unrotated Factors (F1 to F7) representing Aeroradiospectrometric Data (Table 3),Wadi Dib Area, Northern Eastern Desert, Egypt

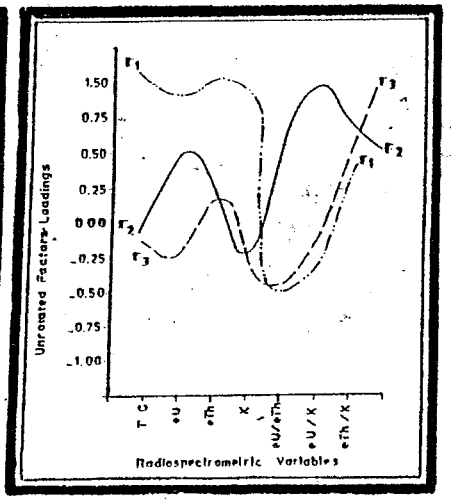

Fig. (13) : Unrotated Factor Loadings (Table 3) of the various seven Aeroradiospect rometric Variables on each of the First three Unrotated Factors (F1, F2 and F3), Wadi Dib Area, Northern Eastern Desert, Egypt

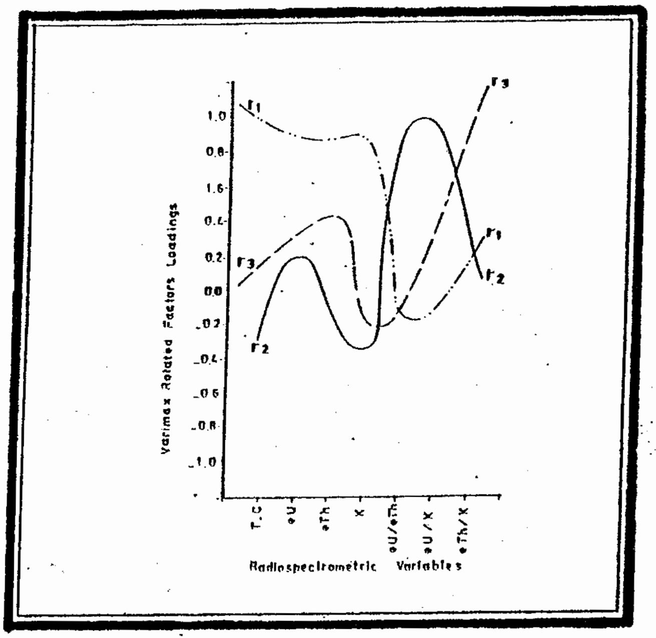

Fig. (14) : Varimax Rotated Factor Loadings (Table 4) of the various Seven Aeroradiospectrometric Variables on each of the First Three Rotated Factors (F1, F2 and F3), Wadi Dib area, Northern Eastern Desert, Egypt

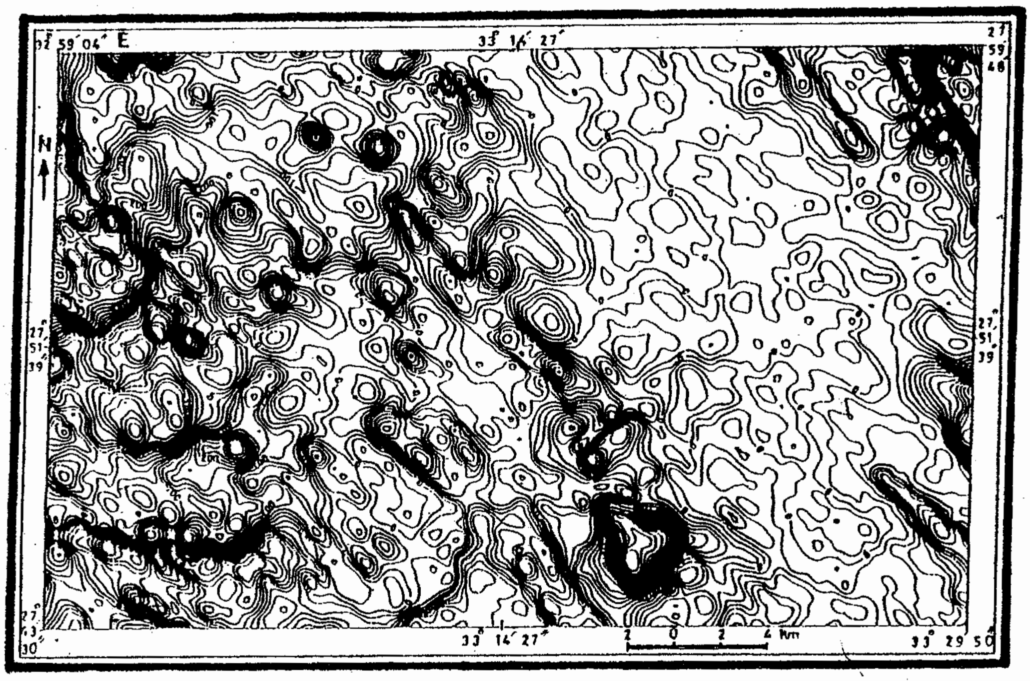

Fig. (15) : Contours of the First Factor (F1) Scores of Wadi Dib area, Northern Eastern Desert, Egypt

(Contour Interval = 20 Scores)

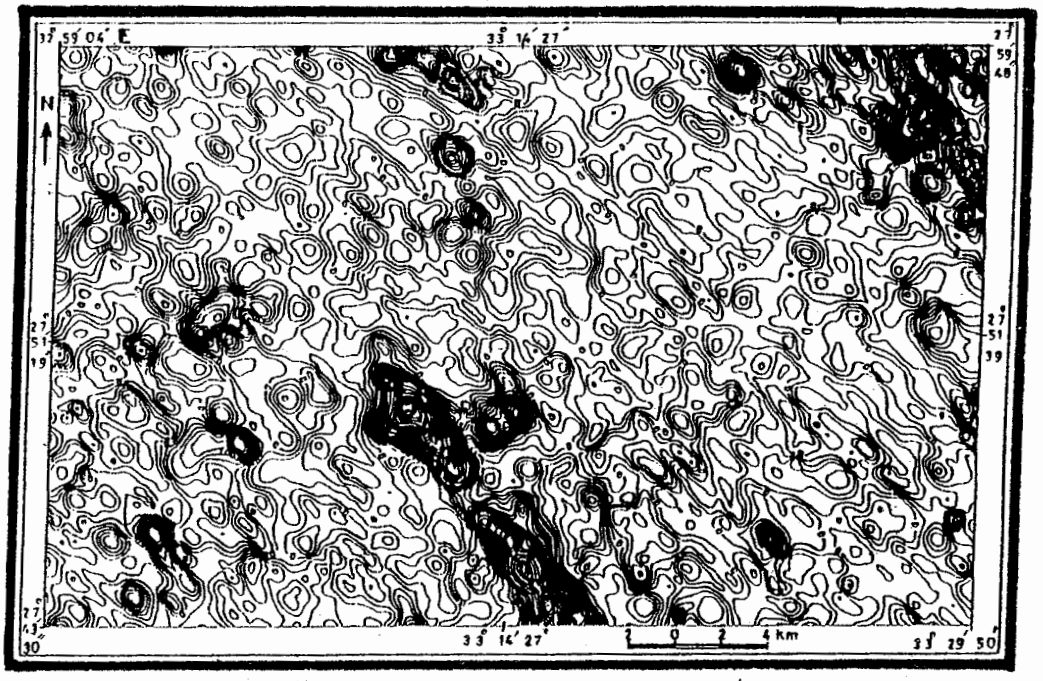

Fig. (16) : Contours of the Second Factor (F2) Scores of Wadi Dib area, Northern Eastern Desert, Egypt

(Contour Interval = 50 Scores)

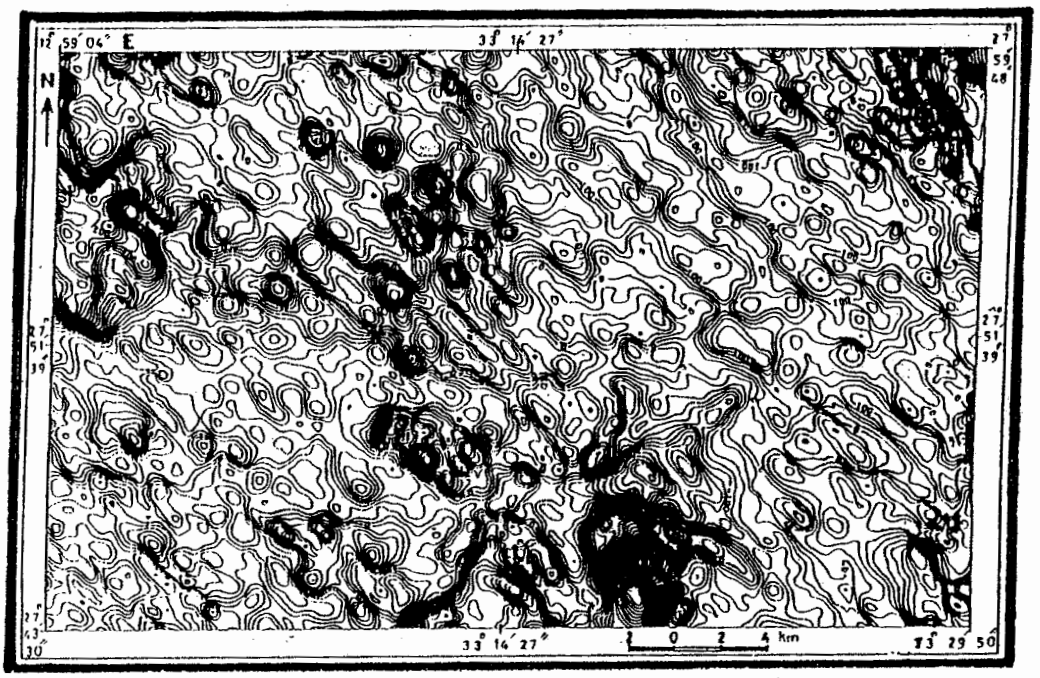

Fig. (17) : Contours of the Third Factor (F3) Scores of Wadi Dib area, Northern Eastern Desert, Egypt

(Contour Interval = 50 Scores)

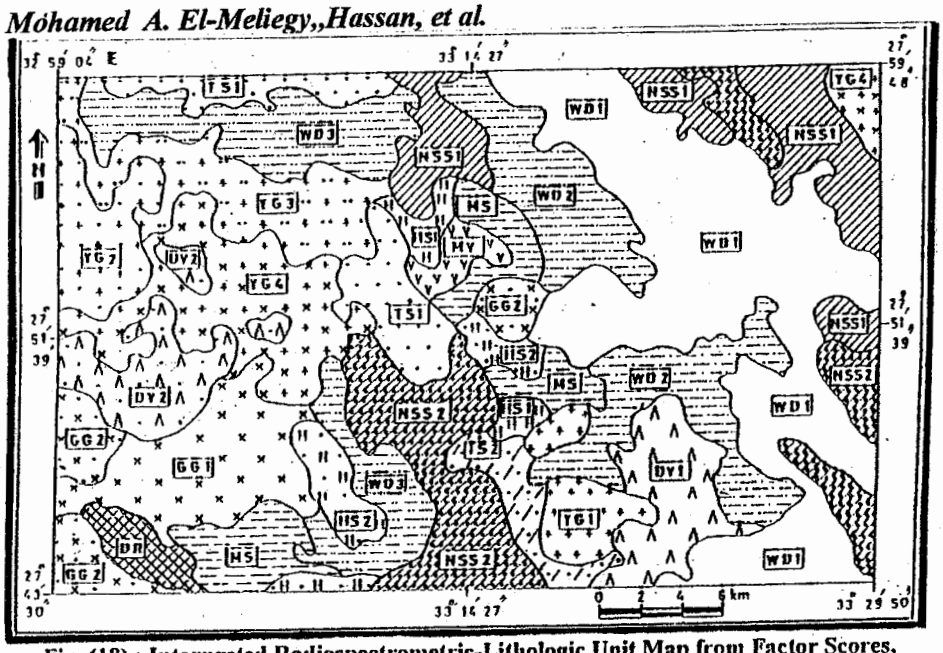

Fig. (18) : Interpreted Radiospectrometric-Lithologic Unit Map from Factor Scores, Wadi Dib Area, Northern Eastern Desert, Egypt

LEGEND

: WD -1	Quaternary	: YG - 1		: DV-1	Dokhan
: WD -2	(Wadi Sediments)	: YG - 2	Younger	: DV-2	Volcanics
: WD -3		: YG - 3	Granites	: GG-1	Older
: TS - 1	Tertiary Sediments	: YG - 4		: GG-2	Granitoids
: TS - 2		: IIS - 1	Hammamat	: D R	Diorite-Epidiorite Rocks
: NSS -1	Cretaceous Nubian	: IIS - 2	Sediments	: M V	Metavolcanics
: NSS -2	Sandstones			: M S	Metasediments

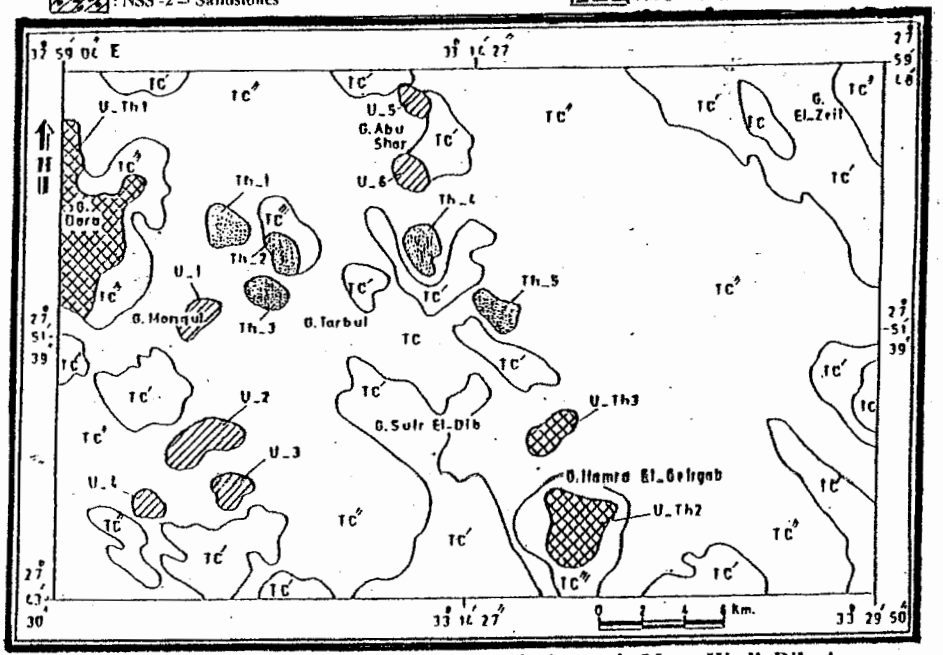

Fig. (19) : Interpreted Aeroradiospectrometric Anomaly Map, Wadi Dib Area, Northern Eastern Desert, Egypt

LEGEND

TC : Low Radioactivity Level	: Mixed Uranium & Thorium (U+Th) Anomaly
TC' : Intermediate Radioactivity Level	: Uranium (U) Anomaly
TC'' : High Radioactivity Level	: Thorium (Th) Anomaly
TC''' : Very High Radioactivity Level	: Boundary Line

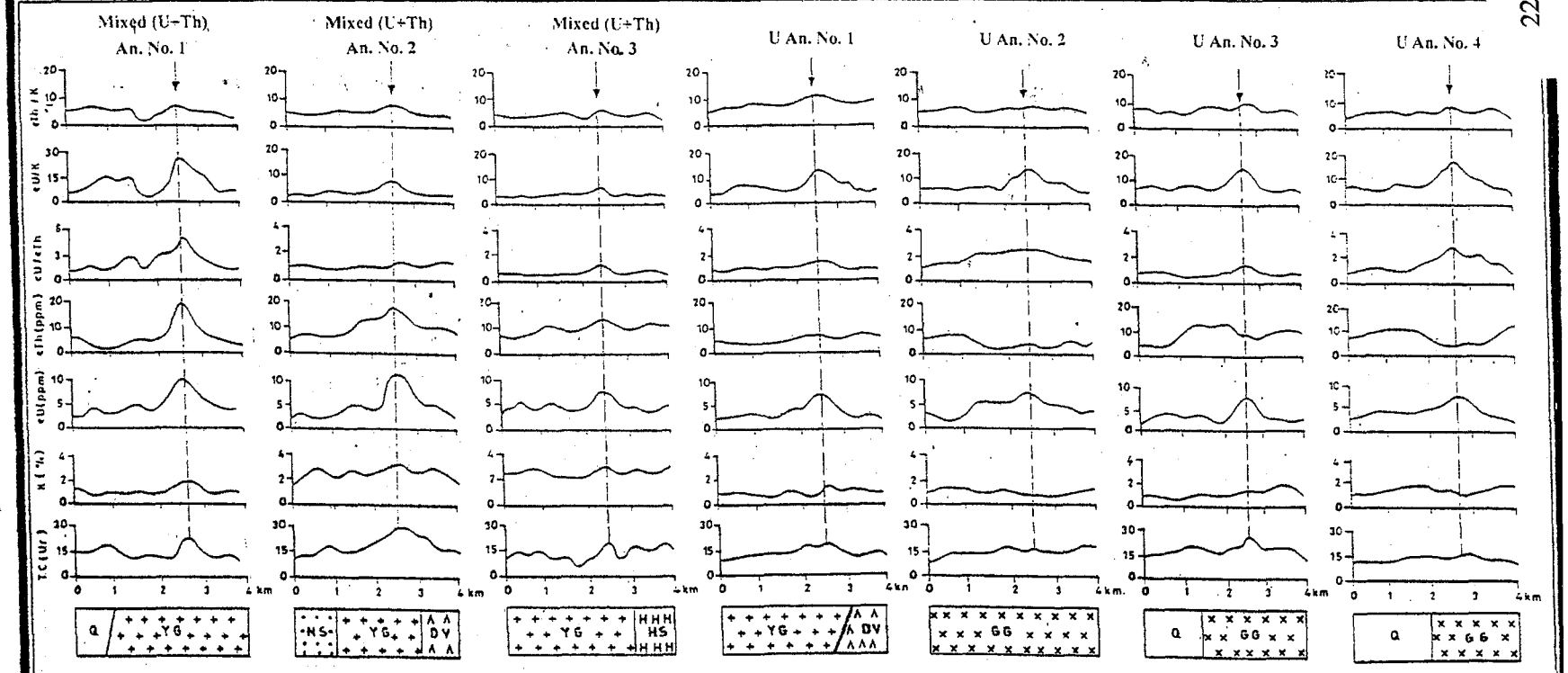

Fig. (20) : Composite Aeroradiospectrometric Stacked Profiles of Mixed Uranium and Thorium (U+Th) Anomalies (An.) Nos. 1, 2 and 3 and Uranium (U) Anomalies (An.) Nos. 1, 2, 3 and 4, Wadi Dib Area, Northern Eastern Desert, Egypt

LEGEND

+++ : YG : Younger Granites
ΛΛΛ : DV : Dokhan Volcanics
XXX : GG : Older Granites
HHH : HS : Hammamat Sediments
Q : Q : Wadi Sediments
- - - - : NS : Nubian Sandstones
/ : Fault

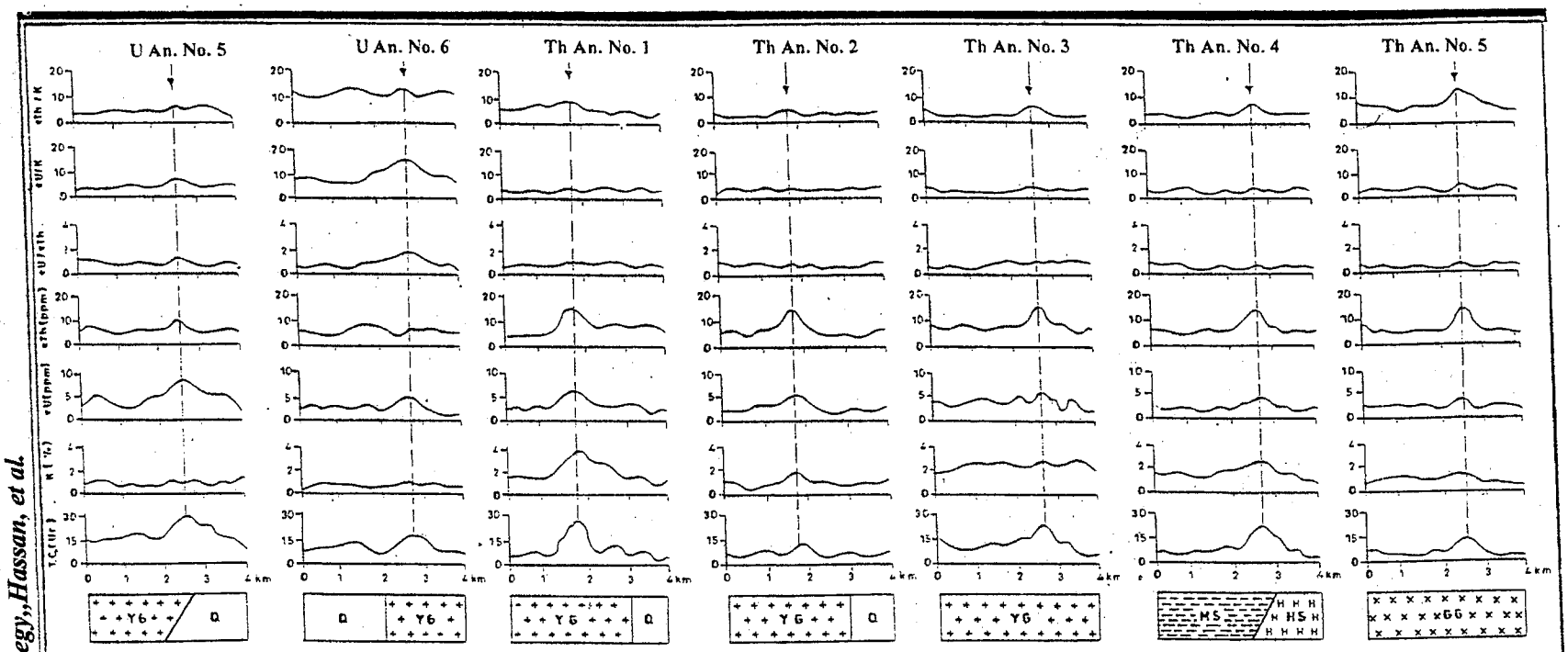

Fig. (21) : Composite Aeroradiospectrometric Stacked Profiles of Uranium (U) Anomalies (An.) Nos. 5 and 6 and Thorium (Th) Anomalies (An.) Nos. 1, 2, 3, 4 and 5, Wadi Dib area, Northern Eastern Desert, Egypt

LEGEND

+++ : Y G : Younger Granites
Q : Q : Wadi Sediments
MS : MS : Metasediments
HHH : H S : Hammamat Sediments
XXX : G G : Older Granites
/ : Fault

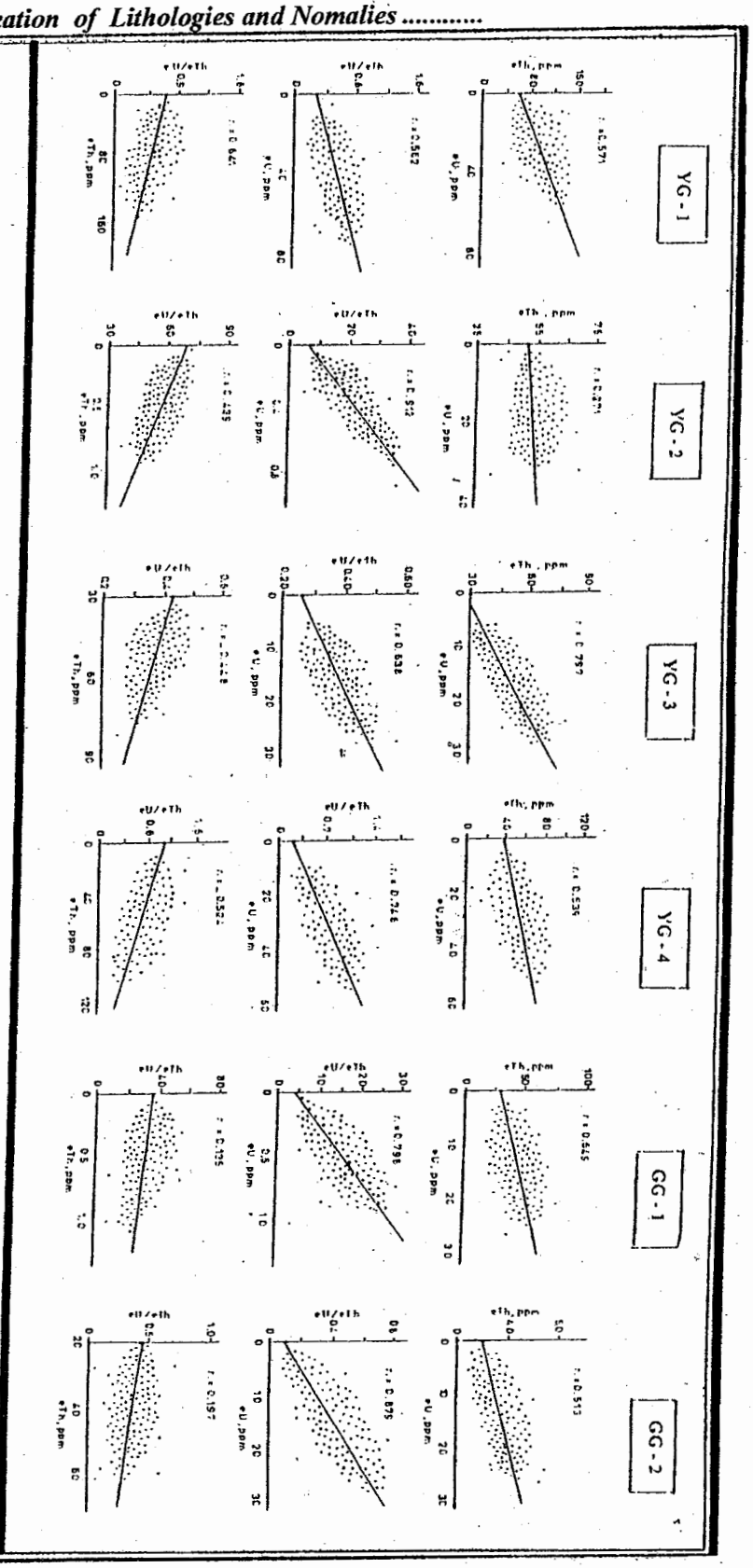

Fig. (22) : Variations of eU and eTh with their Ratios for Younger Granites (YG -1, YG - 2, YG - 3 and YG - 4) and Older Granites (GG -1 and GG - 2), Wadi Dib area, Northern Eastern Desert, Egypt

LEGEND

r = Correlation Coefficient (Computed) cr = Critical Correlation Coefficient at the 95 % level of confidence